J|A|C|S ARTICLES

Published on Web 08/13/2010

Dinitrogen Complexation and Extent of N≡N Activation within the Group 6 "End-On-Bridged" Dinuclear Complexes, $\{(\eta^5\text{-}C_5Me_5)M[N(i\text{-}Pr)C(Me)N(i\text{-}Pr)]\}_2(\mu\text{-}\eta^1\text{:}\eta^1\text{-}N_2)$ (M = Mo and W)

Philip P. Fontaine,[†] Brendan L. Yonke, Peter Y. Zavalij, and Lawrence R. Sita*

Department of Chemistry and Biochemistry, University of Maryland, College Park, Maryland 20742

Received January 18, 2010; E-mail: lsita@umd.edu

Abstract: Chemical reduction of Cp*M[N(i-Pr)C(Me)N(i-Pr)]Cl_3 (Cp* = η^5-C_5Me_5) (**1**, M = Mo) and (**2**, M = W) using 0.5% NaHg in THF provided excellent yields of the diamagnetic dinuclear end-on-bridged dinitrogen complexes $\{Cp^*M[N(i\text{-}Pr)C(Me)N(i\text{-}Pr)]\}_2(\mu\text{-}\eta^1\text{:}\eta^1\text{-}N_2)$ (**6**, M = Mo) and (**8**, M = W), respectively. Chemical reduction of Cp*Mo[N(i-Pr)C(NMe_2)N(i-Pr)]Cl_2 (**4**) with 3 equiv of KC_8 in THF similarly yielded diamagnetic $\{Cp^*Mo[N(i\text{-}Pr)C(NMe_2)N(i\text{-}Pr)]\}_2(\mu\text{-}\eta^1\text{:}\eta^1\text{-}N_2)$ (**7**). Single-crystal X-ray analyses of **7** and **8** confirmed the dinuclear end-on-bridged μ-η^1:η^1-N_2 coordination mode and the solid-state molecular structures of these compounds provided *d*(NN) values of 1.267(2) and 1.277(8) Å for **7** and **8**, respectively. Based on a comparison of ^{15}N NMR spectra for $^{15}N_2$ (99%)-labeled **6** and $^{15}N_2$ (99%)-labeled **8**, as well as similarities in chemical reactivity, a dinuclear μ-η^1:η^1-N_2 structure for **6** is further proposed. For comparison with a first-row metal derivative, chemical reduction of Cp*Ti[N(i-Pr)C(Me)N(i-Pr)]Cl_2 (**9**) with KC_8 in THF was conducted to provide $\{Cp^*Ti[N(i\text{-}Pr)C(Me)N(i\text{-}Pr)]\}_2(\mu\text{-}\eta^1\text{:}\eta^1\text{-}N_2)$ (**10**) for which a *d*(NN) value of 1.270(2) Å was obtained through X-ray crystallography. Compounds **6**−**8** were all found to be thermally robust in toluene solution up to temperatures of at least 100 °C, and **6** and **8** were determined to be inert toward the addition of H_2 or H_3SiPh under a variety of conditions. Single-crystal X-ray analysis of *meso*-$\{Cp^*Mo(H)[N(i\text{-}Pr)C(Me)N(i\text{-}Pr)]\}_2(\mu\text{-}\eta^1\text{:}\eta^1\text{-}N_2)$ (*meso*-**11**), which was serendipitously isolated as a product of attempted alkylation of Cp*Mo[N(i-Pr)C(Me)N(i-Pr)]Cl_2 (**3**) with 2 equiv of *n*-butyllithium, revealed a smaller *d*(NN) value of 1.189(4) Å that is consistent with two Mo(IV,d^2) centers connected by a bridging diazenido, $[\mu\text{-}N_2]^{2-}$, moiety. Moreover, *meso*-**11** was found to undergo clean dehydrogenation in solution at 50 °C to provide **6** via a first-order process. Chemical oxidation of **8** with an excess of $PbCl_2$ in toluene solution at 25 °C provided a 1:1 mixture of *rac*- and *meso*-$\{Cp^*W(Cl)[N(i\text{-}Pr)C(Me)N(i\text{-}Pr)]\}_2(\mu\text{-}\eta^1\text{:}\eta^1\text{-}N_2)$ (**12**); both isomers of which provided solid-state structures through X-ray analyses that are consistent with an electronic configuration comprised of two W(IV,d^2) centers linked through a bridging $[N_2]^{2-}$ group [cf. for *rac*-**12**, *d*(NN) = 1.206(9) Å, and for *meso*-**12**, *d*(NN) = 1.192(3) Å]. Finally, treatment of **6** and **8** with either 4 equiv of CNAr (Ar = 3,5-$Me_2C_6H_3$) or an excess of CO in toluene provided excellent yields of Cp*M[N(i-Pr)C(Me)N(i-Pr)](CNAr)$_2$ (**13**, M = Mo and **14**, M = W) and Cp*M[N(i-Pr)C(Me)N(i-Pr)](CO)$_2$ (**15**, M = Mo and **16**, M = W), respectively. Single-crystal X-ray analyses of **13**−**16**, along with observation of reduced IR vibrational ν_{CN} or ν_{CO} bond-stretching frequencies, provide strong support for the electron-rich character of the Cp*M[N(i-Pr)C(Me)N(i-Pr)] fragment that can engage in a high degree of back-donation with moderate to strong π-acceptors, such as N_2, CNR, and CO. The collective results of this work are analyzed in terms of the possible steric and electronic factors that contribute to preferred mode of μ-N_2 coordination and the extent of N≡N activation, including complete N−N bond scission, within the now completed experimentally-derived ligand-centered isostructural series of $\{Cp^*M[N(i\text{-}Pr)C(Me)N(i\text{-}Pr)]\}_2(\mu\text{-}N_2)$ compounds where M = Ti, Zr, Hf, Ta, Mo, and W.

Introduction

Experimental and theoretical investigations have now conclusively established that substantial N≡N bond elongation of dinitrogen, also referred to as N_2 "activation", can be accomplished through various bridging μ-N_2 coordination modes within different classes of dinuclear complexes of general formula $[L_nM]_2(\mu\text{-}N_2)$, where M is an early transition metal from groups 4−6 of the periodic table.[1−3] A remaining challenge that has proven difficult to overcome, however, is the establishment of a single common supporting ligand platform in which the steric and electronic environment experienced by the metal centers can be held constant while the nature of μ-N_2 coordination and the extent of N≡N activation is allowed to vary as a

[†] Present address: Dow Chemical Company, Freeport, TX.

(1) For reviews, see: (a) Fryzuk, M. D.; Johnson, S. A. *Coord. Chem. Rev.* **2000**, *200*−*202*, 379–409. (b) Shaver, M. P.; Fryzuk, M. D. *Adv. Synth. Catal.* **2003**, *345*, 1061–1076. (c) Gambarotta, S.; Scott, J. *Angew. Chem., Int. Ed.* **2004**, *43*, 5298–5308. (d) MacKay, B. A.; Fryzuk, M. D. *Chem. Rev.* **2004**, *104*, 385–401. (e) MacLachlan, E. A.; Fryzuk, M. D. *Organometallics* **2006**, *25*, 1530–1543. (f) Kuganathan, N.; Green, J. C.; Himmel, H. J. *New. J. Chem.* **2006**, *30*, 1253–1262. (g) Ohki, Y.; Fryzuk, M. D. *Angew. Chem., Int. Ed.* **2007**, *46*, 3180–3183. (h) Chirik, P. J. *Dalton Trans.* **2007**, 16–25. (i) Fryzuk, M. D. *Acc. Chem. Res.* **2009**, *42*, 127–133. (j) Chirik, P. J. *Organometallics* **2010**, *29*, 1500–1517.

Chart 1

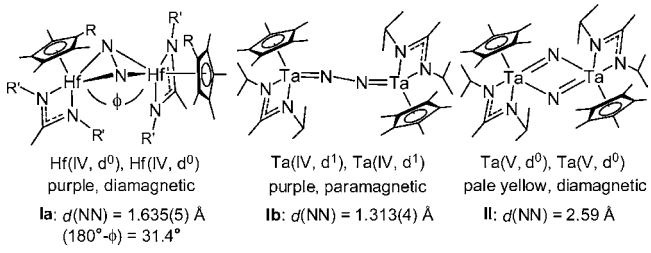

function of the metal's group and row position, formal oxidation state, and d^n electron count.[4] A highly desirable outcome of having ready access to "ligand-centered" isostructural series of $[L_nM]_2(\mu\text{-}N_2)$ complexes is the experimental emergence and successful theoretical analysis of metal-dependent trends for dinitrogen activation that can aid the development of molecular catalysts for the direct hydrogenation of dinitrogen to ammonia that further operate with greater energy efficiencies than that presently required by the high-temperature, high-pressure Haber−Bosch commercial process.[5]

Recently, we have reported that the η^5-cyclopentadienyl/η^2-amidinate (CpAm) ligand combination can be used to access several different group 4 and group 5 dinuclear dinitrogen complexes of general formula $\{(\eta^5\text{-}C_5R_5)M[N(R^1)C(R^2)N(R^3)]\}_2(\mu\text{-}N_2)$ (**I**).[6,7] With the second- and third-row group 4 metals, a "side-on-bridged" $\mu\text{-}\eta^2\text{:}\eta^2\text{-}N_2$ coordination mode is obtained that is characterized by having an extremely large value for the N−N distance parameter, *d*(NN), that further correlates with the degree of nonplanarity of the M_2N_2 four-membered ring that is defined by the generic structure depicted in Chart 1 for the series of compounds represented by $\{(\eta^5\text{-}C_5Me_4R)M[N(R^1)C(R^2)N(R^3)]\}_2(\mu\text{-}\eta^2\text{:}\eta^2\text{-}N_2)$ (**Ia**), where M = Zr or Hf.[8] Indeed, for the specific case of M = Hf, R = R^2 = Me and R^1 = R^3 = Et in **Ia**, the experimentally determined solid-state *d*(NN) value of 1.635(5) Å now appears to be the longest known N−N bond distance within a molecularly discrete $[L_nM]_2(\mu\text{-}N_2)$ compound.[1] For comparison, the corresponding *d*(NN) values for free N_2 and free hydrazine (N_2H_4) are 1.0974 Å and 1.460 Å, respectively.[9] On the other hand, in spite of these extreme values for *d*(NN) in **Ia**, retention of a N−N bonding interaction in these diamagnetic compounds is consistent with a ground-state electronic structure in which two M(IV,d^0) centers are linked through a highly reduced, side-on-bridged hydrazido $[\mu\text{-}\eta^2\text{:}\eta^2\text{-}N_2]^{4-}$ moiety. Moreover, an inherent corollary to this formalization is that complete N≡N bond cleavage cannot occur in these compounds as formation of a metal nitrido end-product would require invoking the involvement of an inaccessible M(V) oxidation state for these group 4 metals.

In contrast to group 4 derivatives of **I**, the paramagnetic, third-row, group 5 metal analogue, $\{Cp^*Ta[N(i\text{-}Pr)C(Me)N(i\text{-}Pr)]\}_2(\mu\text{-}\eta^1\text{:}\eta^1\text{-}N_2)$ ($Cp^* = \eta^5\text{-}C_5Me_5$) (**Ib**), was found to adopt the "end-on-bridged" $\mu\text{-}\eta^1\text{:}\eta^1\text{-}N_2$ coordination mode shown in Chart 1 in which two formal M(IV,d^1) centers are connected in linear fashion through a highly reduced $[\mu\text{-}N_2]^{4-}$ bridge.[7] Surprisingly, however, although **Ib** possesses a smaller solid-state *d*(NN) value of 1.313(4) Å, this compound quantitatively converts in solution at temperatures above 0 °C to the dinuclear bis(μ-nitrido) species $\{Cp^*Ta[N(i\text{-}Pr)C(Me)N(i\text{-}Pr)(\mu\text{-}N)]\}_2$ (**II**), the structure of which is also depicted in Chart 1. The solid-state *d*(NN) value of 2.59 Å obtained for the planar $[M(\mu\text{-}N)]_2$ four-membered ring of **II** provides strong evidence that complete N−N bond cleavage has occurred with concomitant generation of two M(V,d^0) metal centers during the **Ib** → **II** thermal process.[6,10]

With successful results for group 4 and group 5 metal derivatives of **I** in hand, a reasonable next step to undertake in our efforts was to attempt to extend the experimental structural database of compounds to include group 6 metal analogues. Herein, we now report the successful realization of this goal that serves to establish an important ligand-based isostructural series for $\{Cp^*M[N(i\text{-}Pr)C(Me)N(i\text{-}Pr)]\}_2(\mu\text{-}N_2)$ in which M can now be an early transition metal chosen from among the group 4 (M = Ti, Zr, and Hf), group 5 (M = Ta), and group 6 (M = Mo and W). Through comparisons of the solid-state structures, thermal stabilities, and chemical reactivities of these various derivatives of **I**, it is now possible to contemplate the nature of the steric and electronic factors of the CpAm ligand platform that govern the preference for a particular metal/$\mu\text{-}N_2$ coordination mode combination, the extent of N≡N activation, and specific details of reaction energy profiles that are associated

(2) For recent experimental studies related to dinuclear N_2 activation leading to complete N−N bond cleavage, see: (a) Akagi, F.; Matsuo, T.; Kawaguchi, H. *Angew. Chem., Int. Ed.* **2007**, *46*, 8778–8781. (b) Nikiforov, G. B.; Vidyaratne, I.; Gambarotta, S.; Korobkov, I. *Angew. Chem., Int. Ed.* **2009**, *48*, 7415–7419. (c) Knobloch, D. J.; Lobkovsky, E.; Chirik, P. J. *Nat. Chem.* **2010**, *2*, 30–35.

(3) For relevant theoretical studies, see: (a) Fryzuk, M. D.; Haddad, T. S.; Mylvaganam, M.; McConville, D. H.; Rettig, S. J. *J. Am. Chem. Soc.* **1993**, *115*, 2782–2792. (b) Cui, Q.; Musaev, D. G.; Svensson, M.; Sieber, S.; Morokuma, K. *J. Am. Chem. Soc.* **1995**, *117*, 12366–12367. (c) Khoroshun, D. V.; Musaev, D. G.; Morokuma, K. *Organometallics* **1999**, *18*, 5653–5660. (d) Basch, H.; Musaev, D. G.; Morokuma, K. *Organometallics* **2000**, *19*, 3393–3403. (e) Pool, J. A.; Bernskoetter, W. H.; Chirik, P. J. *J. Am. Chem. Soc.* **2004**, *126*, 14326–14327. (f) Bobadova-Parvanova, P.; Wang, Q.; Morokuma, K.; Musaev, D. G. *Angew. Chem., Int. Ed.* **2005**, *44*, 7101–7103. (g) Studt, F.; MacKay, B. A.; Fryzuk, M. D.; Tuczek, F. *Dalton Trans.* **2006**, 1137–1140. (h) Graham, D. C.; Beran, G. J. O.; Head-Gordon, M.; Christian, G.; Stranger, R.; Yates, B. F. *J. Phys. Chem. A* **2005**, *109*, 6762–6772. (i) Martinez, S.; Morokuma, K.; Musaev, D. G. *Organometallics* **2007**, *26*, 5978–5986. (j) Tanaka, H.; Shiota, Y.; Matsuo, T.; Kawaguchi, H.; Yoshizawa, K. *Inorg. Chem.* **2009**, *48*, 3875–3881.

(4) For instance, for a homologous series of transition metal dinuclear N_2 complexes, see: (a) Chomitz, W. A.; Arnold, J. *Chem.Commun* **2007**, 4797–4799. For lanthanide metals, see: (b) Evans, W. J.; Fang, M.; Zucchi, G.; Furche, F.; Ziller, J. W.; Hoekstra, R. M.; Zink, J. I. *J. Am. Chem. Soc.* **2009**, *131*, 11195–11202, and references cited therein.

(5) (a) Travis, T. *Chem. Ind.* **1993**, *15*, 581–585. (b) Appl, M. *Chem. Tech.* **1994**, *46*, 125–135. (c) Smil, V. *Enriching the Earth: Fritz Haber, Carl Bosch, and the Transformation of World Food Production*; MIT Press: Cambridge, MA, 2001. (d) Smil, V. *Nature* **1999**, *401*, 429. (e) DOE/EIA-0484 Report, International Energy Outlook, 2007; OIAF: Washington, DC, 2007.

(6) Hirotsu, M.; Fontaine, P. P.; Zavalij, P. Y.; Sita, L. R *J. Am. Chem. Soc.* **2007**, *129*, 12690–12692.

(7) Hirotsu, M.; Fontaine, P. P.; Epshteyn, A.; Zavalij, P. Y.; Sita, L. R. *J. Am. Chem. Soc.* **2007**, *129*, 9284–9285.

(8) For discussions of the electronic and steric factors that govern "side-on-bridged" $\mu\text{-}\eta^2\text{:}\eta^2\text{-}N_2$ complexation within group 4 dinuclear $[L_nM]_2(\mu\text{-}N_2)$ complexes, see refs 1g−j, 3a, and d and references cited therein.

(9) (a) Wilkinson, P. G.; Houk, N. B. *J. Chem. Phys.* **1956**, *24*, 528. (b) Sutton, L. E., Ed.; *Tables of Interatomic Distances and Configurations in Molecules and Ions*; Chemical Society Special Publications; The Chemical Society: London, 1958, Vol. 11.

(10) For other early transition metal $[M(\mu\text{-}N)]_2$ compounds obtained through formal dinitrogen activation and N−N bond cleavage, see: (a) Haddad, T. S.; Aistars, A.; Ziller, J. W.; Doherty, N. M. *Organometallics* **1993**, *12*, 2420–2422. (b) Clentsmith, G. K. B.; Bates, V. M. E.; Hitchcock, P. B.; Cloke, F. G. N. *J. Am. Chem. Soc.* **1999**, *121*, 10444–10445. (c) Caselli, A.; Solari, E.; Scopelliti, R.; Floriani, C.; Re, N.; Rizzoli, C.; Chiesi-Villa, A. *J. Am. Chem. Soc.* **2000**, *122*, 3652–3670. (d) Fryzuk, M. D.; Kozak, C. M.; Bowdridge, M. R.; Patrick, B. O.; Rettig, S. J. *J. Am. Chem. Soc.* **2002**, *124*, 8389–8397.

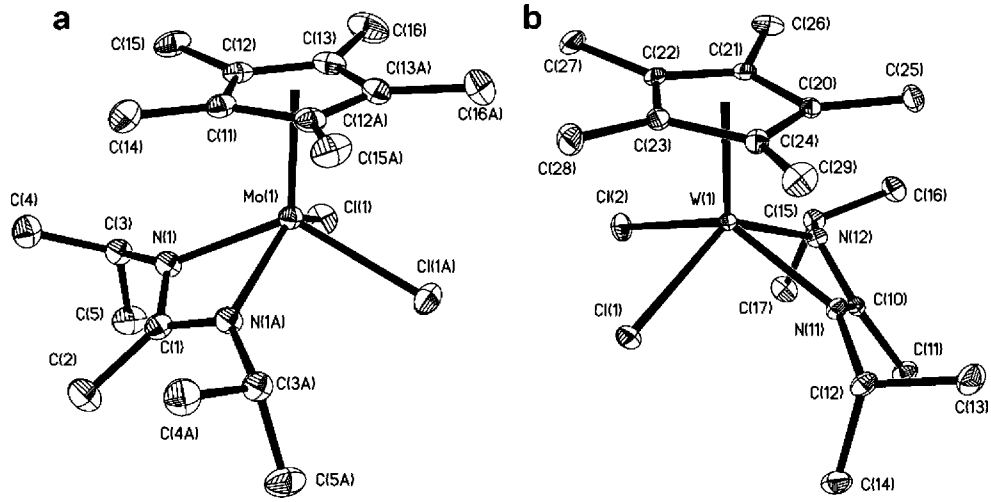

Figure 1. Molecular structure (30% thermal ellipsoids) of (a) **3** and (b) **5**. Hydrogen atoms have been removed for the sake of clarity.[14]

Scheme 1

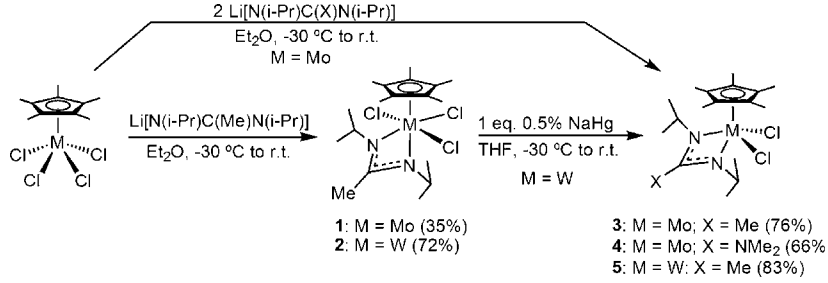

with complete N−N bond cleavage and N-atom functionalization processes.

Results

A. Synthesis of Cp*M[N(i-Pr)C(X)N(i-Pr)]Cl$_n$ (M = Mo and W, X = Me or NMe$_2$, n = 2 or 3). Scheme 1 summarizes the synthetic methods that were employed in the present work to obtain group 6 metal chloride complexes that could serve as viable precursors to the corresponding derivatives of **I** through chemical reduction.[6,7] To begin, synthesis of the M(V,d^1) trichlorides, Cp*M[N(i-Pr)C(Me)N(i-Pr)]Cl$_3$, where M = Mo (**1**) and W (**2**), proceeded with good yields through reaction of the respective Cp*MCl$_4$ starting materials[11] with 1 equiv of the lithium amidinate salt, Li[N(i-Pr)C(Me)N(i-Pr)]; the latter reagent being readily prepared through the addition of methyl lithium to *N*,*N*-diisopropylcarbodiimide and subsequently isolated in pure form. Although **1** and **2** were eventually discovered to be excellent precursors to the desired dinuclear μ-N$_2$ complexes, it was initially thought that higher yields might be ensured through chemical reduction of the corresponding M(IV,d^2) dichloride precursors. As Scheme 1 reveals, a very practical route to Cp*M[N(i-Pr)C(X)N(i-Pr)]Cl$_2$ for M = Mo involved a "one-pot" procedure starting from Cp*MoCl$_4$ that employs a second equivalent of Li[N(i-Pr)C(X)N(i-Pr)] as an *in situ* sacrificial reductant. In this way, compounds **3** (X = Me) and **4** (X = NMe$_2$) were readily prepared in small but sufficient quantities for synthetic evaluation. On the other hand, for M = W, the best means to obtain compound **5** (X = Me) in high yields was determined to be through chemical reduction of the trichloride **2** using 1 equiv of 0.5% sodium amalgam (NaHg) in tetrahydrofuran (THF) according to Scheme 1.

Although not extensively relied upon in the present work, the group 6 dichloride compounds **3** and **5** are proving to be useful for exploring a broader range of midvalent group 6 organometallic chemistry. These compounds also now complete a ligand-centered isostructural series for Cp*M[N(i-Pr)C(X)N(i-Pr)]Cl$_2$ that spans the early transition metal series and, more specifically, where M = Ti, Zr[6], Hf[6], Ta[7], Mo, and W. Since, to the best of our knowledge, CpMo[N(Ph)C(H)N(Ph)]Cl$_2$ (Cp = η^5-C$_5$H$_5$) previously represented the only known example of a group 6 metal CpAm derivative,[12] compounds **3** and **5** were subjected to further study. In this regard, both compounds proved to be thermally stable in solution and the solid-state for extended periods of time. In solution, both of the molybdenum derivatives, **3** and **4**, were found to be high-spin and paramagnetic, while the third-row tungsten congener **5** is low-spin and diamagnetic, and these observations are consistent with expectations for a square-pyramidal ligand-field geometry for a 16-electron, M(IV,d^2) complex.[13] Single-crystal X-ray analyses of **3** and **5** confirmed the geometry of the structures depicted in Scheme 1 and Figure 1 further presents a side-by-side comparison of the respective solid-state molecular structures.[14] In brief, the gross structural features of **3** and **5** are geometrically similar to those

(11) (a) Murray, R. C.; Blum, L.; Liu, A. H.; Schrock, R. R. *Organometallics* **1985**, *4*, 953–954. (b) Gomez, S. P.; Jiménez, I.; Martín, A.; Perdraz, T.; Royo, P.; Sellés, A.; Vázquez de Miguel, A. *Inorg. Chim. Acta* **1998**, *273*, 270–278.

(12) Romao, C. C.; Royo, B. *J. Organomet. Chem.* **2002**, *663*, 78–82.

(13) (a) Poli, R. *Chem. Rev.* **1996**, *96*, 2135–2204. (b) Baker, R. T.; Calabrese, J. C.; Harlow, R. L.; Williams, I. D. *Organometallics* **1993**, *12*, 830–841.

(14) Details are provided in the Supporting Information.

Scheme 2

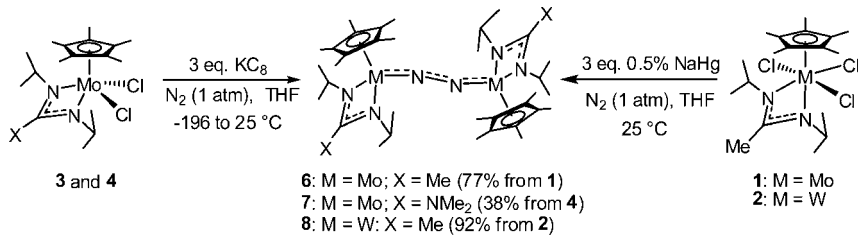

that we have previously reported for a number of related group 4 and group 5 Cp*M[N(R^1)C(X)N(R^2)]Cl$_2$ derivatives.[15] Between the two structures, the metal-related bond length and bond angle metrical parameters for **3** and **5** are also quite similar [cf. for **3** Mo(1)−N(1) = 2.112(3) Å, Mo(1)−Cl(1) = 2.4104(9) Å, N(1)−Mo(1)−N(1A) = 61.31(14)°, Cl(1)−Mo(1)−Cl(1A) = 86.59(5)°; for **5** W(1)−N(11) = 2.0707(15) Å, W(1)−N(12) = 2.0764(15) Å, W(1)−Cl(1) = 2.4130(5) Å, W(1)−Cl(2) = 2.4215(5) Å, N(11)−W(1)−N(12) = 63.27(6)°, Cl(1)−W(1)−Cl(2) = 83.221(17)°]. However, the structure of the tungsten derivative **5** displays a significant nonplanarity associated with the four-membered ring amidinate fragment, as evidenced by a value of 21.1° for the angle between the two planes defined by N(11)−W(1)−N(12) and N(11)−C(10)−N(12), whereas the corresponding angle in **3** is only 5.1°. A possible manifestation of this amidinate ring nonplanarity for **5** appears in the ^{1}H NMR (400 MHz, benzene-d_6, 25 °C) spectrum of this compound in which the resonance at δ 4.02 ppm for the methyl group of the amidinate fragment, NC(C*H*$_3$)N, is shifted far downfield from the expected chemical shift range of 1.4−1.6 ppm that is typically observed for the group 4 analogues.[15]

B. Synthesis and Solution Characterization of {Cp*M[N(i-Pr)C(X)N(i-Pr)]}$_2$(μ-η^1:η^1-N$_2$) (M = Ti, Mo, and W, X = Me or NMe$_2$). Following our previously published synthetic procedure,[6,7] we first sought to obtain the desired group 6 derivatives of **I** through chemical reductions of the respective M(IV,d^2) dichlorides **3**−**5**. Accordingly, as Scheme 2 presents, chemical reduction of either of the molybdenum compounds, **3** or **4**, at low temperature under an atmosphere of N$_2$ using 3 equiv of potassium graphite (KC$_8$) in THF, provided, in both cases, a modest yield of a diamagnetic, yellow-brown crystalline material for which ^{1}H NMR and elemental (C, H, and N) analyses were fully consistent with formation of the expected {Cp*Mo[N(i-Pr)C(X)N(i-Pr)]}$_2$(μ-N$_2$) products, where X = Me (**6**) and X = NMe$_2$ (**7**), respectively. It was subsequently determined, however, that direct chemical reduction of the trichloride **1** employing 3 equiv of 0.5% NaHg in THF at 25 °C reproducibly provided a high yield of **6**, and accordingly, this latter route became the preferred one for conveniently accessing larger quantities of this material. In similar fashion, the tungsten trichloride **2** could also be reduced with 3 equiv of 0.5% NaHg in THF according to Scheme 2 to provide a 92% yield of a forest green, crystalline, diamagnetic compound for which ^{1}H NMR and elemental analyses were once again fully consistent with the empirical formula expected for the desired product {Cp*W[N(i-Pr)C(Me)N(i-Pr)]}$_2$(μ-N$_2$) (**8**).

Although group 6 metal derivatives of **I** were the primary target goal of the present study, with the availability of

Scheme 3

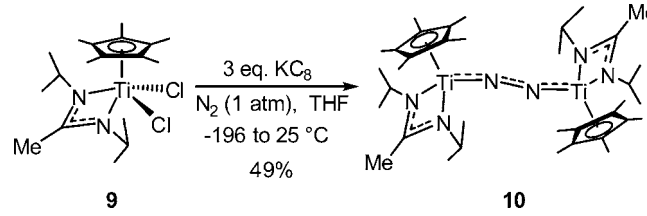

Cp*Ti[N(i-Pr)C(Me)N(i-Pr)]Cl$_2$ (**9**) that was prepared as part of another investigation, the opportunity presented itself to attempt the synthesis of a first-row group 4 analogue of **I** where M = Ti. Thus, as Scheme 3 reveals, low-temperature chemical reduction of **9** employing 3 equiv of KC$_8$ in THF did, in fact, provide a gratifying 49% yield of a dark green, diamagnetic crystalline material for which ^{1}H NMR and elemental analyses were satisfactorily consistent with the expected formulation for {Cp*Ti[N(i-Pr)C(Me)N(i-Pr)]}$_2$(μ-N$_2$) (**10**).

C. Solid-State Molecular Structures of {Cp*M[N(i-Pr)-C(X)N(i-Pr)]}$_2$(μ-η^1:η^1-N$_2$) (M = Ti, Mo, and W; X = Me or NMe$_2$) (7, 8, and 10). Unfortunately, due to high solubility in pentane and poor crystallinity, single crystals of compound **6** suitable for crystallographic analysis could not be obtained even after expending considerable effort. Thus, the main purpose for including the η^2-guanidinate, [N(i-Pr)C(NMe$_2$)N(i-Pr)], series of compounds, **4** and **7**, in the present study was to possibly obtain a crystalline analogue of **6** that would be suitable for X-ray crystallography. Fortunately, single-crystals of **7** did, indeed, prove to be much more amenable for X-ray analysis, as did those for compounds **8** and **10**. Figures 2−4 provide the solid-state molecular structures of **7**, **8**, and **10**, respectively, while Table 1 presents a compilation of the selected metrical

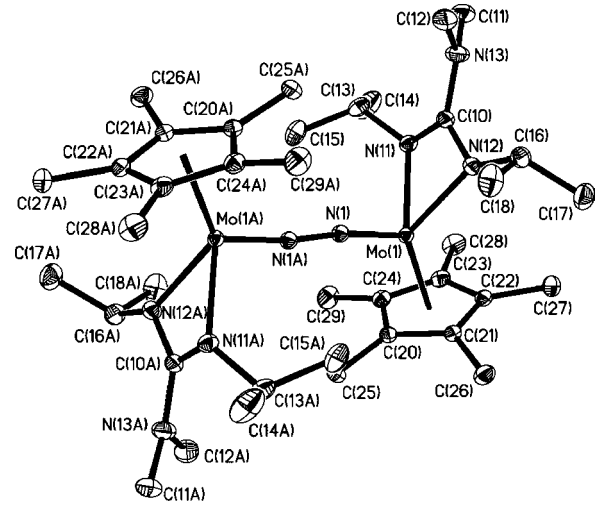

Figure 2. Molecular structure (30% thermal ellipsoids) of **7**. Hydrogen atoms have been removed for the sake of clarity.[14]

(15) See, for instance: (a) Sita, L. R.; Babcock, J. R. *Organometallics* **1998**, *17*, 5228–5230. (b) Zhang, Y.; Reeder, E. K.; Keaton, R. J.; Sita, L. R. *Organometallics* **2004**, *23*, 3512–352. (c) Kissounko, D. A.; Fettinger, J. C.; Sita, L. R. *Inorg. Chim. Acta* **2003**, *345*, 121–129. (d) Epshteyn, A.; Zavalij, P. Y.; Sita, L. R. *J. Am. Chem. Soc.* **2006**, *128*, 16052–16053.

Table 1. Comparison of MNNM Structural Parameters for $[L_nM]_2(\mu\text{-}\eta^1\text{:}\eta^1\text{-}N_2)$ Complexes

compound	*d*(MN) (Å)	*d*(NN) (Å)	*θ*(MNN) (deg)	ref
7	1.7944(12)	1.267(2)	171.26(15)	this work
8	1.816(4)	1.277(8)	176.7(5)	this work
8[a]	1.720(8)	1.402(17)	177.4(11)	this work
10	1.7749(18), 1.7741(18)	1.270(2)	166.71(15), 166.96(16)	this work
meso-**11**	1.899(2)	1.189(4)	167.4(3)	this work
meso-**12**	1.9032(17)	1.192(3)	169.0(2)	this work
rac-**12**	1.885(7)	1.206(9)	177.7(6)	this work
Ib	1.807(2)	1.313(4)	172.7(3)	7
$\{[(t\text{-}Bu)ArN]_3Mo\}_2(\mu\text{-}N_2)$ (**III**)	1.870(2), 1.872(2)	1.217(2)	179.87(14)	16c
[**III**][$B(Ar^F)_4$]	1.835(3), 1.841(1)	1.239(4)		16c
[**III**][$B(Ar^F)_4$]$_2$	1.798(2)	1.265(5)		16c
$\{Cp^*Me_3Mo\}_2(\mu\text{-}N_2)$	1.819(2), 1.821(3)	1.236(3)	172.0(2)	17e
$\{Cp^*Me_3W\}_2(\mu\text{-}N_2)$	1.742(17), 1.763(18)	1.334(26)	167.0(16) 170.2(16)	17b, c
$\{[R_3SiN_3N]Mo\}_2(\mu\text{-}N_2)$	1.907(8)	1.20(2)	178(1)	17g
$\{[Ar'N_3N]Mo\}_2(\mu\text{-}N_2)$	1.930(4)	1.186(7)	178.9(5)	17i
$\{[NpN_3N]W\}_2(\mu\text{-}N_2)$	1.845(11)	1.39(2)		17j
$[W(PhC{\equiv}CPh)(dme)Cl_2(\mu\text{-}N_2)$	1.776(11), 1.735(11)	1.292(16)	175.6(10)	17a

[a] Obtained as a 1:1 cocrystal with *meso*-**12**.[14]

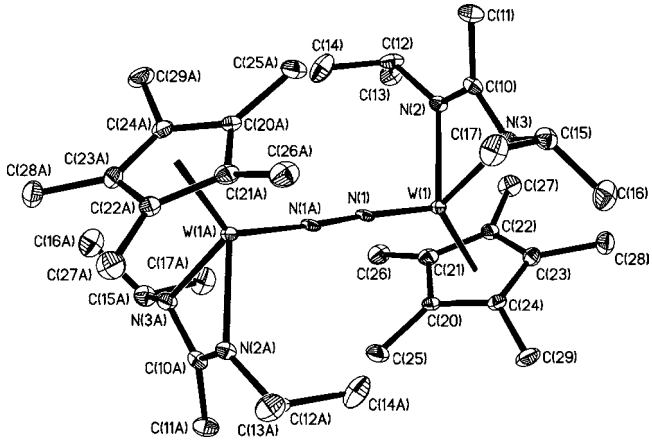

Figure 3. Molecular structure (30% thermal ellipsoids) of **8**. Hydrogen atoms have been removed for the sake of clarity.[14]

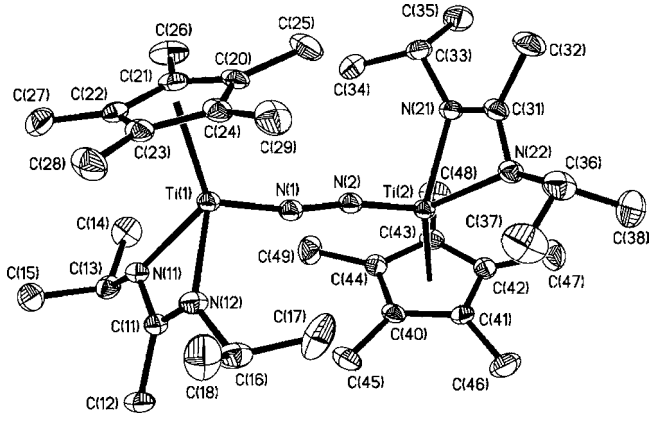

Figure 4. Molecular structure (30% thermal ellipsoids) of **10**. Hydrogen atoms have been removed for the sake of clarity.[14]

parameters for the M−N−N−M framework of these structures, along with those for several other second- and third-row group 6 dinuclear $[L_nM]_2(\mu\text{-}N_2)$ complexes that have appeared in the literature.[16,17] As is readily apparent from a quick survey of the figures, all the new compounds, **7**, **8**, and **10**, were found to exist in the solid state as a dinuclear end-on-bridged $\mu\text{-}\eta^1\text{:}\eta^1\text{-}N_2$ coordination complex in which the M−N−N−M framework adopts a slight transoid "zigzag" conformation in a manner similar to that previously discovered for the group 5 analogue **Ib**.[7] On the other hand, **7**, **8**, and **10** all display somewhat smaller *d*(NN) values of 1.267(2), 1.277(8), and 1.270(2) Å, respectively, compared with that observed for **Ib** [*d*(NN) =1.313(4) Å]. Although a more thorough analysis will be presented shortly, the observed *d*(NN) bond lengths for **7**, **8**, and **10** qualitatively imply that a moderate degree of N≡N activation is present within the ground-state structures of these compounds.[1,16−18]

D. Solution Structures and Thermal Stabilities of $\{Cp^*M[N(i\text{-}Pr)C(X)N(i\text{-}Pr)]\}_2(\mu\text{-}\eta^1\text{:}\eta^1\text{-}N_2)$ (M = Mo and W; X = Me or NMe_2) (6−8). In order to assist with structural assignments in solution, $^{15}N_2$-labeled **6** and $^{15}N_2$-labeled **8** were

(16) (a) Laplaza, C. E.; Cummins, C. C. *Science* **1995**, *268*, 861–863. (b) Laplaza, C. E.; Johnson, M. J. A.; Peters, J. C.; Odom, A. L.; Kim, E.; Cummins, C. C.; George, G. N.; Pickering, I. J. *J. Am. Chem. Soc.* **1996**, *118*, 8623–8638. (c) Curley, J. J.; Cook, T. R.; Reece, S. Y.; Müller, P.; Cummins, C. C. *J. Am. Chem. Soc.* **2008**, *130*, 9394–9405.

(17) (a) Churchill, M. R.; Li, Y. J.; Theopold, K. H.; Schrock, R. R. *Inorg. Chem.* **1984**, *23*, 4472–4476. (b) Murray, R. C.; Schrock, R. R. *J. Am. Chem. Soc.* **1985**, *107*, 4557–4558. (c) Churchill, M. R.; Li, Y. J. *J. Organomet. Chem.* **1986**, *301*, 49–59. (d) O'Regan, M. B.; Liu, A. H.; Finch, W. C.; Schrock, R. R.; Davis, W. M. *J. Am. Chem. Soc.* **1990**, *112*, 4331–4338. (e) Schrock, R. R.; Kolodziej, R. M.; Liu, A. H.; Davis, W. M.; Vale, M. G. *J. Am. Chem. Soc.* **1990**, *112*, 4338–4345. (f) O'Regan, M. B.; Liu, A. H.; Finch, W. C.; Schrock, R. R.; Davis, W. M. *J. Am. Chem. Soc.* **1990**, *112*, 4331–4338. (g) Shih, K. Y.; Schrock, R. R.; Kempe, R.; Davis, W. M. *J. Am. Chem. Soc.* **1994**, *116*, 8804–8805. (h) Kol, M.; Schrock, R. R.; Kempe, R.; Davis, W. M. *J. Am. Chem. Soc.* **1994**, *116*, 4382–4390. (i) Greco, G. E.; Schrock, R. R. *Inorg. Chem.* **2001**, *40*, 3861–3878. (j) Scheer, M.; Müller, J.; Schiffer, M.; Baum, G.; Winter, R. *Chem.—Eur. J.* **2000**, *6*, 1252–1257.

(18) (a) Bercaw, J. E. *J. Am. Chem. Soc.* **1974**, *96*, 5087–5095. (b) Sanner, R. D.; Duggan, D. M.; McKenzie, T. C.; Marsh, R. E.; Bercaw, J. E. *J. Am. Chem. Soc.* **1976**, *98*, 8358–8365. (c) de Wolf, J. M.; Blaauw, R.; Meetsma, A.; Teuben, J. H.; Gyepes, R.; Varga, V.; Mach, K.; Veldman, N.; Spek, A. L. *Organometallics* **1996**, *15*, 4977–4983. (d) Hagadorn, J. R.; Arnold, J. *J. Am. Chem. Soc.* **1996**, *118*, 893–894. (e) Beydoun, N.; Duchateau, R.; Gambarotta, S. *J. Chem. Soc., Chem. Commun.* **1992**, 244–246. (f) Mullins, S. M.; Duncan, A. P.; Bergman, R. G.; Arnold, J. *Inorg. Chem.* **2001**, *40*, 6952–6963. (g) Hanna, T. E.; Keresztes, I.; Lobkovsky, E.; Bernskoetter, W. H.; Chirik, P. J. *Organometallics* **2004**, *23*, 3448–3458. (h) Morello, L.; Yu, P. H.; Carmichael, C. D.; Patrick, B. O.; Fryzuk, M. D. *J. Am. Chem. Soc.* **2005**, *127*, 12796–12797. (i) Scherer, A.; Kollak, K.; Luetzen, A.; Friedmann, M.; Haase, D.; Saak, W.; Beckhaus, R. *Eur. J. Inorg. Chem.* **2005**, 1003–1010. (j) Bai, G.; Wei, P.; Stephan, D. W. *Organometallics* **2006**, *25*, 2649–2655. (k) Hanna, T. E.; Bernskoetter, W. H.; Bouwkamp, M. W.; Lobkovsky, E.; Chirik, P. J. *Organometallics* **2007**, *26*, 2431–2438. (l) Hanna, T. E.; Lobkovsky, E.; Chirik, P. J. *Organometallics* **2009**, *28*, 4079–4088. Also, see: (m) Walter, M. D.; Sofield, C. D.; Andersen, R. A. *Organometallics* **2008**, *27*, 2959–2970.

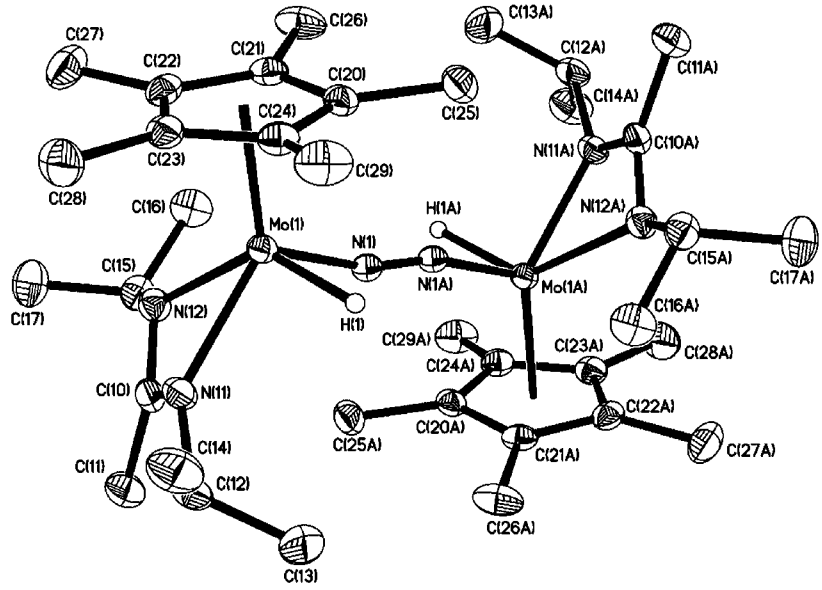

Figure 5. Molecular structure (30% thermal ellipsoids) of *meso*-**11**. Hydrogen atoms have been removed for the sake of clarity except those for Mo(1) and Mo(1A), which are represented by small spheres of arbitrary size.[14]

Scheme 4

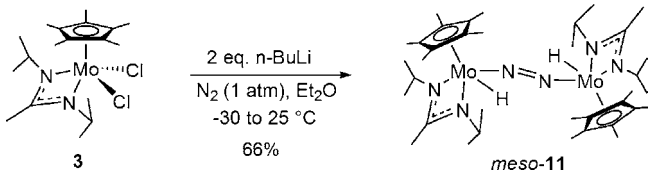

prepared from **3** and **2**, respectively, by performing the low-temperature KC_8 chemical reductions of Scheme 2 under an atmosphere of $^{15}N_2$ (99%)-labeled N_2. A $^{15}N\{^1H\}$ NMR (40.5 MHz, benzene-d_6, liq. NH_3 as an external reference) spectrum of $^{15}N_2$-labeled **6** obtained in this manner displayed a single ^{15}N resonance with a chemical shift of δ 375 ppm, while that for $^{15}N_2$-labeled **8** likewise revealed a single ^{15}N resonance with a chemical shift of δ 351.4 ppm that was now further flanked by two sets of ^{183}W satellites [$^1J(^{183}W-^{15}N) = 145$ Hz and $^2J(^{183}W-^{15}N) = 10.5$ Hz] in a manner that is most consistent with a linear dinuclear end-on-bridged $^{183}W-^{15}N-^{15}N-^{183}W$ spin system. Although not conclusive evidence, the observed similarities in the ^{15}N chemical shifts for $^{15}N_2$-labeled **6** and $^{15}N_2$-labeled **8** strongly suggests that the former compound also exists as a dinuclear end-on-bridged μ-η^1:η^1-N_2 coordination complex, at least in solution. Further support for this structural assignment is provided by considering that the chemical reactivity profiles for **6** and **8**, which will be presented herein, are so far identical in nature.

Of particular interest is that in contrast to the low thermal stability displayed in solution by the group 5 derivative **Ib**, compounds **6**−**8** are all thermally robust, and they remain unchanged upon heating in toluene solution at 100 °C for 18 h as determined by ^1H NMR spectroscopy. This high degree of thermal stability of **6**−**8** also stands in sharp contrast to {[(t-Bu)ArN]$_3$Mo}$_2$(μ-η^1:η^1-N_2) (Ar = 3,5-$Me_2C_6H_3$) (**III**), which has been shown to undergo complete N−N bond cleavage in solution at subambient temperatures to generate 2 equiv of the terminal nitride species [[(t-Bu)ArN]$_3$Mo≡N.[16] A further intriguing aspect of this difference in stability is that both **7** and **8** possess *d*(NN) values that are significantly larger than that of **III**, which is only 1.217(2) Å as recently reported by Cummins and co-workers (see Table 1).[16c] The disparity in stability among **7**, **8**, and **III** serves as another reminder that bond length and bond strength do not correlate in a simple fashion and one must consider the broader picture of the potential energy landscape for a compound, including the depth of energy minima, in order to best assess the origin of stability. Finally, as a side note, a high degree of stability in solution was found to extend to the first-row group 4 metal derivative **10** as well.

E. Synthesis and Structural Characterization of {Cp*M(X)[N(i-Pr)C(X)N(i-Pr)]}$_2$(μ-η^1:η^1-N_2) (M = Mo, X = H and M =W, X = Cl) (11 and 12). During the course of investigations conducted to explore the chemical reactivity of the group 6 metal dichlorides **3** and **5**, two dinuclear CpAm complexes closely related to **I** were serendipitously discovered, and accordingly, details of these compounds are included here as well. To begin, as presented in Scheme 4, reaction of **3** with 2 equiv of *n*-butyllithium in diethyl ether (Et_2O) provided a 66% yield of the dinuclear end-on-bridged μ-η^1:η^1-N_2 dihydride species *meso*-{Cp*Mo(H)[N(i-Pr)C(Me)N(i-Pr)]}$_2$(μ-η^1:η^1-N_2) (**11**) as a diamagnetic, crystalline material. Figure 5 displays the solid-state molecular structure derived from single crystals of *meso*-**11** that were obtained through fractional crystallization and subjected to single-crystal X-ray analysis.[14] Table 1 also includes for comparison purposes the following metrical parameters for the Mo−N−N−Mo framework of this structure: Mo(1)−N(1), 1.899(2) Å, N(1)−N(1A), 1.189(4) Å, and N(1A)-N(1)−Mo(1), 167.4(3)°.[14] Here, the larger *d*(MN) and smaller *d*(NN) values observed for *meso*-**11**, compared with the corresponding values for **7**, are strongly supportive of a ground-state electronic configuration for the former compound that consists of two Mo(IV,d^2) centers that are now being linked through a bridging diazenido, [μ-N_2]$^{2-}$, moiety as depicted in Scheme 4.

As Scheme 5 reveals, partial chemical reduction of the tungsten trichloride **2** with 2.5 equiv of KC_8 in THF produced a complex mixture of products that included dichloride **5**, **8**, and a set of two new diastereomeric compounds that were eventually revealed through X-ray crystallography to be *rac,meso*-{Cp*W(Cl)[N(i-Pr)C(Me)N(i-Pr)]}$_2$(μ-η^1:η^1-N_2) (**12**). Single crystals that were isolated from recrystallization of this complex mixture at −30 °C were shown by X-ray analysis to

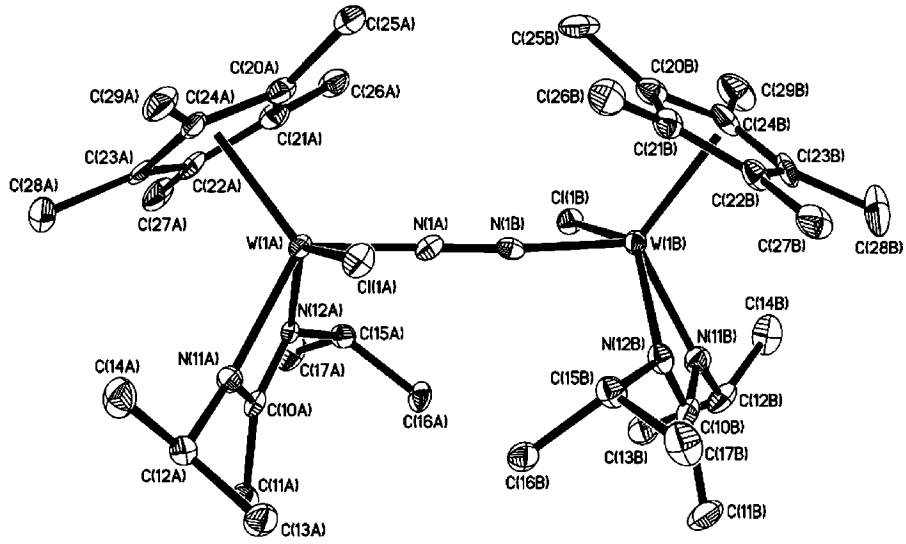

Figure 6. Molecular structure (30% thermal ellipsoids) of *rac*-**12**. Hydrogen atoms have been removed for the sake of clarity.[14]

Scheme 5

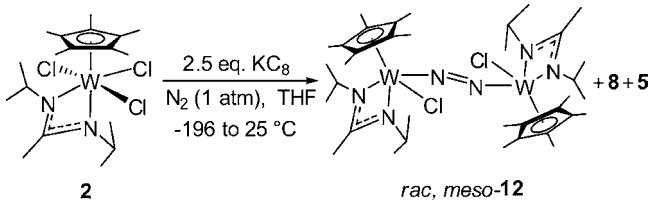

possess a unit cell comprised of **8** and *rac*-**12** in a 1: 1 ratio. More intriguingly, structural parameters associated with **8** within this 1: 1 cocrystal exhibited smaller *d*(MN) values and a significantly larger *d*(NN) value than those determined for pure **8** [cf., 1.720(8) Å and 1.402(17) Å, respectively] (see Table 1). The occurrence of two substantially different sets of *d*(MN) and *d*(NN) values for **8** presumably arises as the result of subtle differences in crystal packing forces, and this observation can further be taken as strong evidence that **8**, and perhaps other third-row dinuclear μ-N_2 complexes as well, resides in a relatively shallow minimum on the potential energy surface with respect to W−N and N−N bond length distortions.

Figure 6 presents the molecular structure of *rac*-**12** for which the following bond length and bond angle metrical parameters were determined: W(1)−N(1), 1.885(7) Å; N(1)−N(1A), 1.206(9) Å; and N(1A)−N(1)−W(1), 177.7(6)°.[14] Once again, based on the relative magnitudes of these bond length parameters for the W−N−N−W framework of *rac*-**12**, vis-a-vis the corresponding values for **8**, a formal ground-state electronic structure for the former compound can be assigned that consists of two W(IV,d^2) metal centers that are connected through an intervening diazenido, $[\mu\text{-}N_2]^{2-}$, bridge as depicted in Scheme 5.

F. Chemical Reactivity of {Cp*M[N(i-Pr)C(Me)N(i-Pr)]}$_2$(μ-η^1:η^1-N_2) (M = Mo and W) (6 and 8). Given some ambiguity that exists regarding the formal oxidation state of the metal centers in the diamagnetic compounds, **6**−**8**, and more specifically, whether to consider them to be M(II,d^4) or M(IV,d^2) (*vide infra*), a preliminary survey of the chemical reactivity of the isostructural analogues **6** and **8** was undertaken. To begin, in light of the successful isolation and structure determination of *meso*-**11**, as well as our prior report that the group 5 derivative **Ib** undergoes clean "1,4-addition" of H_2 at 0 °C to yield *rac*,*meso*-{Cp*Ta(H)[N(i-Pr)C(Me)N(i-Pr)]}$_2$(μ-η^1:η^1-N_2) (**IV**) for which a *d*(NN) value of 1.307(6) Å was obtained,[7]

Scheme 6

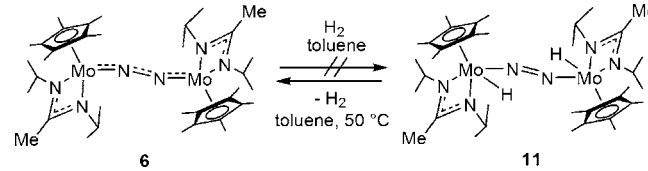

Scheme 7

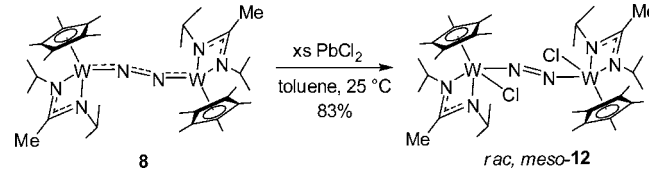

hydrogenations of **6** and **8** were separately attempted in toluene solution at temperatures within the range of 25 to 90 °C within a sealed NMR tube. Unfortunately, as Scheme 6 presents, both compounds remained inert and unchanged under all hydrogenation conditions investigated. On the other hand, during the course of these studies, it was determined that *meso*-**11** readily undergoes thermal conversion to **6** in toluene solution at 50 °C through a process that is first-order in both disappearance of starting material and appearance of product. An Eyring analysis of this **11** → **6** transformation, conducted using variable-temperature ^{1}H NMR within a flame-sealed NMR tube, yielded activation parameters of $\Delta H^{\ddagger} = 35.3$ kcal mol^{-1} and $\Delta S^{\ddagger} = 27.4$ eu. Although evolution of H_2 was not directly observed, the positive entropic value is consistent with a mechanistic pathway in which overall elimination of H_2 occurs. Finally, although previous success was achieved with the hydrosilylation of both group 4 and group 5 derivatives of **I**,[6,7] compound **6** remained inert toward H_3SiPh in toluene solution up to temperatures of 90 °C, while a mixture of **8** and H_3SiPh produced a complex mixture of products after several days in toluene at 50 °C.

As presented in Scheme 7, treatment of compound **8** with an excess of $PbCl_2$ in toluene at 25 °C provided an 83% yield of a 1:1 diastereomeric mixture of *rac*- and *meso*-**12**, from which pure single crystals of *meso*-**12** were obtained for X-ray analysis through fractional crystallization at −30 °C. Figure 7 provides the solid-state molecular structure of *meso*-**12** for which the

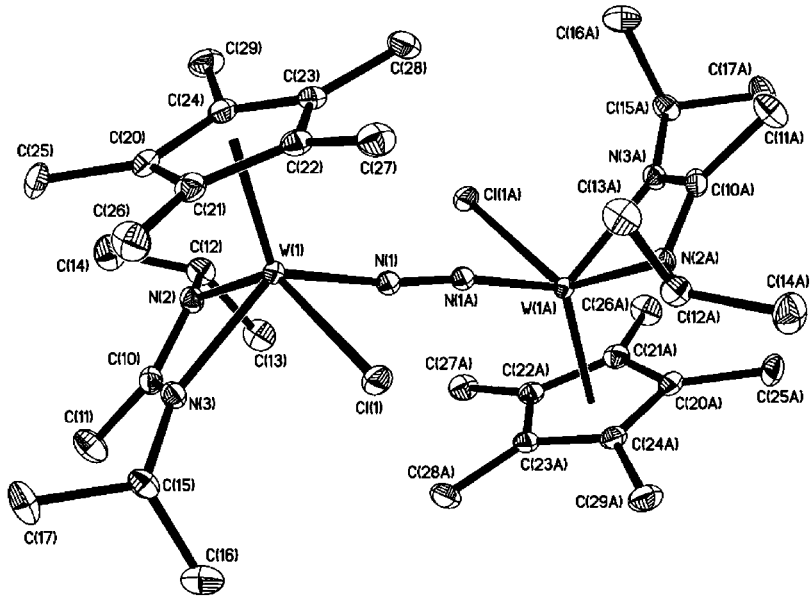

Figure 7. Molecular structure (30% thermal ellipsoids) of *meso*-**12**. Hydrogen atoms have been removed for the sake of clarity.[14]

Scheme 8

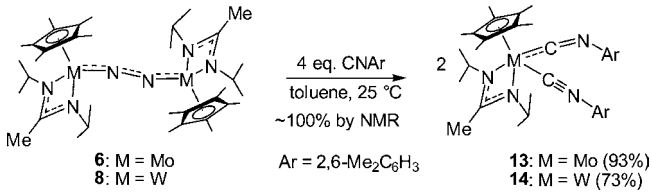

following metrical parameters were obtained: W(1)−N(1), 1.9032(17)Å; N(1)−N(1A), 1.192(3) Å; and N(1A)−N(1)−W(1), 169.0(2)°.[14] Once again, the smaller *d*(NN) value observed for *meso*-**12** relative to that of **8** is in keeping with a diazenido, $[\mu\text{-}N_2]^{2-}$, group in this compound that is bridging two W(IV, d^2) centers.

As part of a screen for group transfer and insertion chemistry, it was discovered that both **6** and **8** reacted cleanly in toluene solution with 4 equiv of the isocyanide, C≡NAr (Ar = 2,6-$Me_2C_6H_3$), to provide excellent isolated yields of the diamagnetic, crystalline bis(isocyanide) products, **13** and **14**, respectively, according to Scheme 8. This process is most likely driven forward by the greater π-acceptor character of an isocyanide ligand, compared with that of dinitrogen,[19] but here it is also interesting to note that utilization of only 2 equiv of CNAr cleanly provided a 1:1 mixture of starting material and product, with no evidence for any intermediates or other side products as established by ^{1}H NMR spectroscopy. Although a detailed kinetic analysis of this ligand substitution reaction has not yet been undertaken, it is reasonable to assume that simultaneous coordination and competing back-donation of the first 2 equiv of CNAr to **6** or **8** (i.e., one isocyanide per metal center) is required to reduce π-back-donation from the metal to the μ-N_2 group to the extent that the latter can then be rapidly displaced by the next 2 equiv of CNAr. Single-crystal X-ray analyses of **13** and **14** further support the strong π-acceptor character of the isocyanide ligands that are engaged in a high degree of back-donation from the metal.[14] Moreover, each compound displays a significant deviation from nonlinearity of the C−N−C_{aryl} bond angles of the two metal-bonded CNAr ligands, one of which possesses a C−N−C_{aryl} bond angle of 142.0(2)° in **13** and a corresponding value of 139.2(3)° in **14**. In contrast, a more obtuse bond angle is associated with the other CNAr group [cf. a C−N−C_{aryl} value of 167.2(3)° in **13** and 163.2(3)° in **14**]. Such bond angle distortions for isocyanide ligands have previously been attributed to a strong π-acceptor character in which back-donation of electron density from the metal into an antibonding π*-orbital of the C≡NR bond occurs.[20] In keeping with this π-acceptor model, the solution infrared spectra of **13** and **14** in pentane exhibited two reduced vibrational carbon−nitrogen bond-stretching modes associated with the CNAr ligands at ν_{CN} = 1971 and 1966 cm^{-1} for **13** and at ν_{CN} = 1952 and 1940 cm^{-1} for **14**. Finally, despite the C_1-symmetric nature of these compounds in the solid-state, ^{1}H and ^{13}C{^{1}H} NMR spectroscopy support a dynamic process in solution that provides a structure of higher C_s-symmetry in which the two isocyanide groups become structurally (magnetically) equivalent.

The interaction of **6** and **8** with other strong π-acceptors was further explored, and gratifyingly, it was discovered that both compounds react rapidly with an excess of carbon monoxide in toluene solution at room temperature to provide good yields of the diamagnetic crystalline bis(carbonyl) derivatives, **15** and **16**, according to Scheme 9. Once again, single-crystal X-ray analyses served to confirm the structural assignments that are depicted in the scheme.[14] Solid-state infrared spectra (KBr) for **15** and **16** exhibit two reduced vibrational carbon−oxygen bond-stretching modes associated with the CO ligands at ν_{CO} = 1909 and 1806 cm^{-1} for **15** and at ν_{CO} = 1892 and 1788 cm^{-1} for **16**. For comparison, the IR spectrum of $[Cp_2Mo(CO)_2][BF_4]_2$ is characterized by ν_{CO} = 2139 and 2108 cm^{-1} and that for $CpMo(\eta^3\text{-}C_5H_5)(CO)_2$ by ν_{CO} = 1950 and 1854 cm^{-1}.[21] Similar ν_{CO} values are reported for the tungsten congeners of these two compounds, namely, ν_{CO} = 2133 and 2087 cm^{-1} for

(19) Pombeiro, A. J. L.; Chatt, J.; Richards, R. L. *J. Organomet. Chem.* **1980**, *190*, 297–304.

(20) (a) Martins, A. M.; Calhorda, M. J.; Romão, C. C.; Völkl, C.; Kiprof, P.; Filippou, A. C. *J. Organomet. Chem.* **1992**, *423*, 367–390. (b) Filippou, A. C.; Dias, A. R.; Martins, A. M.; Romão, C. C. *J. Organomet. Chem.* **1993**, *455*, 129–135.

(21) Ascenso, J. R.; de Azevedo, C. G.; Goncalves, I. S.; Herdtweck, E.; Moreno, D. S.; Pessanha, M.; Romão, C. C. *Organometallics* **1995**, *14*, 3901–3919.

Scheme 9

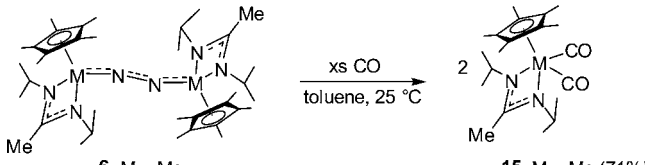

6: M = Mo
8: M = W

15: M = Mo (71%)
16: M = W (59%)

$[Cp_2W(CO)_2][BF_4]_2$ and ν_{CO} = 1955 and 1872 cm^{-1} for $CpW(\eta^3\text{-}C_5H_5)(CO)_2$.[22] Hence, these collective data support the conclusion that the Cp*M[N(i-Pr)C(Me)N(i-Pr)] fragment is formally quite electron-rich and it can engage in a very strong degree of π-back-donation with π-acceptor ligands, such as CNR and CO.

Discussion

The collective set of compounds experimentally synthesized and characterized for $\{Cp^*M[N(i\text{-}Pr)C(Me)N(i\text{-}Pr)]\}_2(\mu\text{-}N_2)$ now encompasses M = Ti (**10**), Zr (**Ic**),[6] Hf (**Id**),[6] Ta (**Ib**),[7] Mo (**6**), and W (**8**). Importantly, this group represents perhaps the most comprehensive series of ligand-centered isostructural $[L_nM]_2(\mu\text{-}N_2)$ complexes yet reported that span across the entire early transition metals and that has representation from the first-row down to the third-row metals. Not surprisingly, analyses of solid-state structures and physiochemical properties that are associated with this set of compounds are beginning to uncover qualitative metal-dependent trends that may prove essential for understanding the role of steric and electronic factors in governing the mode of μ-N_2 complexation, formal metal oxidation state, and the extent of dinitrogen activation within dinuclear $[L_nM]_2(\mu\text{-}N_2)$ complexes supported by the CpAm ligand set, which in some cases also includes examples of complete N−N bond cleavage and N-atom functionalization processes.[6,7]

A. Side-On Bridging vs End-On Bridging Dinuclear μ-N_2 Coordination. While the steric and electronic effects of the supporting $\eta^5\text{-}C_5Me_5/\eta^2$-[N(i-Pr)C(Me)N(i-Pr)] ligand environment might remain constant, the covalent radii for the metals in this series are in the following order: group 4, Ti (1.60 Å), Zr (1.75 Å) ≈ Hf (1.75 Å); group 5, V (1.53 Å), Nb (1.64 Å), Ta (1.70 Å); group 6, Cr (1.39 Å), Mo (1.54 Å), W (1.62 Å).[23] As Fryzuk[1g,i] and Chirik[1h,j] and co-workers have now amply demonstrated and analyzed for group 4 dinuclear $[L_nM]_2(\mu\text{-}N_2)$ complexes, the extent of nonbonded steric interactions between the ligand environments on the two metal centers can play a critical role in directing the preference for dinuclear side-on-bridged vs end-on-bridged μ-N_2 coordination. Thus, within the steric environment established by the $\eta^5\text{-}C_5Me_5/\eta^2$-[N(i-Pr)C(Me)N(i-Pr)] combination, it appears reasonable to assume that only the second- and third-row group 4 metals, Zr and Hf, are able to accommodate a dinuclear side-on-bridged $\mu\text{-}\eta^2\text{:}\eta^2\text{-}N_2$ bonding motif, whereas the smaller covalent radii for Ti, Ta, Mo, and W now dictate that a dinuclear end-on-bridged $\mu\text{-}\eta^1\text{:}\eta^1\text{-}N_2$ configuration be adopted.[18k,l] Although not yet a target of synthetic effort by us, it is reasonable to predict that the first- and second-row group 5 analogues of $\{Cp^*M[N(i\text{-}Pr)C(Me)N(i\text{-}Pr)]\}_2(\mu\text{-}N_2)$, where M = V and Nb, respectively, should also

Scheme 10

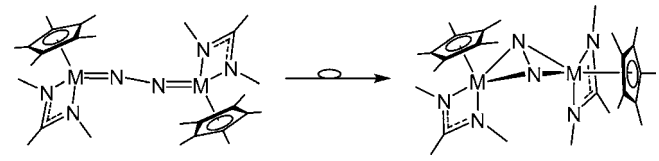

be synthetically accessible, and if so, these should exist in the form of dinuclear end-on-bridged $\mu\text{-}\eta^1\text{:}\eta^1\text{-}N_2$ complexes. On the other hand, a first-row group 6 metal derivative of **I**, where M = Cr, may present a significant synthetic challenge due to a metal covalent radius that is distinctly smaller at 1.39 Å than all the other early transition metals. Indeed, both end-on-bridged and side-on-bridged μ-N_2 dichromium complexes are known, but these remain extremely rare.[24] Moreover, Smith and co-workers[25] have reported that chemical reduction of the CpAm Cr(III) monochloride, $CpCr[N(SiMe_3)C(Ph)N(SiMe_3)]Cl$, under an atmosphere of N_2 *does not* provide a dinitrogen species, but rather simply the Cr(II) product, $CpCr[N(SiMe_3)C(Ph)N(SiMe_3)]$. It remains to be seen, therefore, whether a further decrease in the steric environment of the CpAm ligand set might facilitate μ-N_2 complexation in the case of chromium. A similar strategy is presently being explored to determine whether dinuclear side-on-bridged μ-N_2 derivatives of **I** for Mo and W can likewise be obtained. In this regard, it is interesting to note that the covalent radius of third-row group 5 Ta is only slightly less than that for group 4 Zr and Hf (cf., 1.70 Å and 1.75 Å, respectively). Given this, a possible low-energy pathway for **Ib** leading to N−N bond scission with formation of **II** might actually involve an intramolecular $\mu\text{-}\eta^1\text{:}\eta^1\text{-}N_2 \rightarrow \mu\text{-}\eta^2\text{:}\eta^2\text{-}N_2$ structural isomerization according to Scheme 10. The thermal stability displayed by the group 6 derivatives, **6**−**8**, might then be simply due to an inability to similarly adopt a dinuclear side-on-bridged μ-N_2 structure as the result of steric retardation.

B. Formal Metal Oxidation States for $\{Cp^*M[N(i\text{-}Pr)C(Me)N(i\text{-}Pr)]\}_2(\mu\text{-}N_2)$. A challenging, but useful, exercise related to the investigation of $[L_nM]_2(\mu\text{-}N_2)$ complexes is the assignment of formal metal oxidation states that are a consequence of the extent of N_2 activation that has been achieved. In making this assignment, the qualitative model that is commonly adopted involves the concept of π-back-donation of electron density from the metal orbital into the antibonding molecular orbitals of appropriate symmetry on the μ-N_2 fragment that serves to lower N−N bond order through formal reduction of the N_2 bridge. Based on this model, the extent of μ-N_2 activation reported in the literature for a large variety of $[L_nM]_2(\mu\text{-}N_2)$ complexes ranges from virtually none at all, that is, the μ-N_2 unit is functioning as only a σ-donor to the two metals, to a partially reduced μ-diazenido, $[N_2]^{2-}$, fragment, and finally, to the fully reduced μ-hydrazido, $[N_2]^{4-}$, linkage.[1] Recently, Evans and co-workers[4b] have added yet another member to this spectrum of reduced forms for μ-N_2 with experimental evidence for a bridging radical anion, $\mu\text{-}[N_2]^{3-}$.

(22) Goncalves, I. S.; Romão, C. C. *J. Organomet. Chem.* **1995**, *486*, 155–161.
(23) Cordero, B.; Gomez, V.; Platero-Prats, A. E.; Reves, M.; Echeverria, J.; Cremades, E.; Barragan, F.; Alvarez, S. *Dalton Trans.* **2008**, 2832–2838.
(24) (a) Denholm, S.; Hunter, G.; Weakley, T. J. R. *J. Chem. Soc., Dalton Trans.* **1987**, 2789–2791. (b) Vidyaratne, I.; Scott, J.; Gambarotta, S.; Budzelaar, P. H. M. *Inorg. Chem.* **2007**, *46*, 7040–7049. (c) Monillas, W. H.; Yap, G. P. A.; MacAdams, L. A.; Theopold, K. H. *J. Am. Chem. Soc.* **2007**, *129*, 8090–8091. (d) Berben, L. A.; Kozimor, S. A. *Inorg. Chem.* **2008**, *47*, 4639–4647.
(25) Gallant, A. J.; Smith, K. M.; Patrick, B. O. *Chem. Commun.* **2002**, *23*, 2914–2915.

Scheme 11

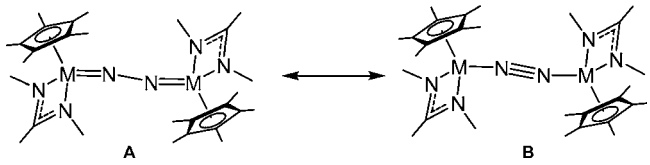

The extreme limit for N_2 activation leading to a fully reduced μ-hydrazido, $[N_2]^{4-}$, bridge is perhaps best represented by the collection of side-on-bridged group 4 derivatives presented by **Ia** in which *d*(NN) values of >1.63 Å would appear to challenge the concept of a N−N bonding interaction.[6,26] However, as previously noted, bond length and bond strength are parameters that do not usually correlate in a simple fashion, and for **Ia**, it is obvious that the M(IV,d^0) metal centers that are intrinsic to the side-on-bridged μ-N_2 structure do not have sufficient electron-reducing equivalents for complete N−N bond scission to occur. Unfortunately, for dinuclear end-on-bridged $[L_nM]_2(\mu$-$N_2)$ complexes, particularly those for which the metal centers have a greater range of formal oxidation states that can be accessed, the common practice of utilizing the value of the experimentally determined *d*(NN) parameter as a measure of the extent of N_2 activation and, from there, as an assessment of formal metal oxidation state, is not a straightforward task due to the spectrum of possibilities that exist between the two limiting resonance structures presented in Scheme 11. Accordingly, reasonable assignments of formal oxidation states for the group 4, group 5, and group 6 derivatives of **I** must be formed with the inclusion and evaluation of additional physiochemical data, such as open vs closed ground-state configurations, thermal stability, accessibility of higher (or lower) oxidation states, and patterns of chemical reactivity. In this fashion, it is reasonable to conclude on the basis of its diamagnetic character and relatively long *d*(NN) value of 1.270(2) Å that the first-row dititanium μ-η^1:η^1-N_2 derivative **10** can best be described as having a spin-coupled delocalized Ti−N−N−Ti framework comprising two Ti(III,d^1) that are linked through a reduced $[N_2]^{2-}$ bridge within the resonance structure **A** of Scheme 11.[18] Likewise, we have previously presented the case that the paramagnetic group 5 derivative **Ib** is also best described as containing two Ta(IV,d^1) centers linked through a highly reduced $[N_2]^{4-}$ bridge. With this formalization, the metal centers in **Ib** still retain sufficient electron-reducing equivalents for final N−N bond cleavage through a low-energy path leading to **II**, which now incorporates two Ta(V,d^0) metal centers in the cleaved product. Moreover, the formal 1,4-addition of H_2 to **Ib** that provides the ditantalum dihydride **IV** as the final product can be viewed as a Ta(IV,d^1) → Ta(V,d^0) metal-centered oxidation that leaves the nature of the μ-$[N_2]^{4-}$ bridge essentially unchanged, as evidenced by the corresponding *d*(NN) values for these two compounds (see Table 1).

In moving to a consideration of the diamagnetic group 6 metal derivatives of **I** represented by compounds **6**−**8**, the question becomes whether these compounds are best described by the ground-state electronic resonance structure **A** that consists of two M(IV,d^2) centers coupled through a bridging $[N_2]^{4-}$ group or, alternatively, the resonance form **B** that is dominated by more reduced metal oxidation states in which two formal M(II,d^4) centers are connected through a less-activated μ-N_2 bridge. Importantly, while the observed *d*(NN) values for **7** and **8** appear to support the former formulation, the chemical reactivity profiles displayed with strong π-acceptors certainly suggest that the bridging μ-N_2 group is easily displaced in **6**−**8**, and accordingly, these compounds can be viewed, to some extent, as viable synthons for M(II,d^4) (M = Mo and W). In reality, the true electronic configuration for **6**−**8** most likely lies somewhere between the two limiting extremes. In this regard, the present work has shown that the Cp*M[N(i-Pr)C(Me)N(i-Pr)] fragment for M = Mo and W can be viewed as a very electron-rich fragment that can engage in a high degree of π-back-donation with moderate to strong π-acceptors, such as N_2, CNR, and CO. Given the magnitude of the *d*(NN) values in **7** and **8**, which support a moderate to strong degree of N_2 activation, the facile displacement of this N_2 bridge by stronger π-acceptors is then equivalent to a formal metal-centered reductive process leading to formation of compounds **13**−**16** that unquestionably possess M(II,d^4) metal centers. The closed-shell electronic structures of **6**−**8** also beg the question of whether a pathway for N−N bond scission might be more accessible starting from an open-shell electronic configuration for group 6 $[L_nM]_2(\mu$-$N_2)$ complexes, as in the case of {[(t-Bu)ArN]$_3$Mo}$_2(\mu$-η^1:η^1-N_2) (**III**), which is best described as being comprised of two formal Mo(V,d^1) metal centers.[16] Here, an evaluation of the one- and two-electron oxidation potentials and oxidation products of **6** and **8** should prove very informative,[17c] and these investigations are currently in progress.

Finally, it is interesting to consider changes in the nature and extent of N_2 activation that arise with chemical transformations involving **6** and **8**. In this respect, the $PbCl_2$-mediated **8** → **12** process can be considered, on the basis of the relative magnitudes of *d*(NN) values (see Table 1), as a formal oxidation of the μ-N_2 group that generates a diazenido linkage of smaller *d*(NN) value in **12** and, thereby, preserves two M(IV,d^2) metal centers. A similar formal oxidation of the μ-N_2 group in {Cp′Hf[N(i-Pr)C(Me)N(i-Pr)]}$_2(\mu$-η^2:η^2-N_2) (Cp′ = η^5-C_5Me_4H) (**Ic**) occurs upon addition of Br_2 to provide {Cp′Hf(Br)[N(i-Pr)C(Me)N(i-Pr)]}$_2(\mu$-η^2:η^2-N_2) (**V**) that likewise possesses a significantly smaller *d*(NN) value consistent with a bridging diazenido group [cf. for **Ic** *d*(NN) = 1.630(4) Å vs for **V** *d*(NN) = 1.253(3) Å].[6]

Conclusion

The CpAm supporting ligand environment is proving to be uniquely versatile for the preparation and experimental investigation of different families of isostructural dinuclear $[L_nM]_2(\mu$-$N_2)$ complexes based on **I** that span the entire set of early transition metals comprising groups 4−6. While not yet ubiquitous for all metals, it is reasonable to assume that synthetic derivatives for M = V and Nb should be accessible, while those for M = Cr may still present a significant challenge. Fortunately, however, the CpAm ligand combination provides for a diverse array of different families of derivatives that can present substituents of varying steric size. Some degree of freedom might also exist for fine-tuning the electronic features of the CpAm platform through substituent modification (e.g., more electron-rich vs more electron-poor). In this respect, the now documented ability of the CpAm ligand environment to support the synthesis, isolation, and characterization of $[L_nM]_2(\mu$-$N_2)$ complexes for metals across the entire early transition metal series establishes a versatile new tool for systematically exploring and analyzing metal-dependent trends that are essential for

(26) It can be noted here that dinitrogen tetroxide, N_2O_4, has a solid-state *d*(NN) value of 1.7562(4) Å that is associated with a N−N bond strength of only 13.6 kcal mol^{-1}, see: Kvick, Å; McMullan, R. K.; Newton, M. D. *J. Chem. Phys.* **1982**, *76*, 3754–3761.

furthering current knowledge regarding dinitrogen activation leading to N−N bond cleavage and N-atom functionalization.

Experimental Section

General Methods. All manipulations with air- and moisture-sensitive compounds were carried out under dinitrogen or argon atmospheres with standard Schlenk or glovebox techniques. All solvents were dried (Na/benzophenone for pentane, Et_2O, toluene, and THF) and distilled under argon prior to use. Benzene-d_6 and toluene-d_8 were dried over Na/K alloy and isolated by vacuum transfer prior to use. Celite was oven-dried (150 °C for several days) before use in the glovebox. Cooling and recrystallizations were performed within the internal freezer of a glovebox. (η^5-C_5Me_5)$MoCl_4$ and (η^5-C_5Me_5)WCl_4 were prepared according to previously reported procedures.[11] ^{1}H NMR and ^{15}N NMR were recorded at 400 and 40.5 MHz respectively, in benzene-d_6 (C_6D_6) or toluene-d_8. ^{15}N NMR chemical shifts are reported relative to liquid ammonia as an external standard. Elemental analyses were carried out by Midwest Microlab.

Synthesis and Characterization of New Compounds. (η^5-C_5Me_5)Mo[N(i-Pr)C(Me)N(i-Pr)]Cl_3 (1). A solution of (η^5-C_5Me_5)$MoCl_4$ (0.626 g, 1.68 mmol) in 100 mL of Et_2O was cooled to −30 °C, whereupon, a solution of Li[N(i-Pr)C(Me)N(i-Pr)] (0.259 g, 1.75 mmol) in 10 mL of Et_2O, precooled to −30 °C, was added dropwise. After the reaction mixture was allowed to warm to room temperature, it was stirred at this temperature for 10.5 h to yield a black-colored solution. The volatiles were removed in vacuo, and then the residue was taken up in a minimum amount of toluene and filtered through a small pad of Celite. The resulting black filtrate was collected, and the solvent was removed once more in vacuo. The crude product was taken up in 10 mL of toluene, to which was added 10 mL of pentane, and the solution was cooled to −30 °C overnight, whereupon 0.284 g of **1** (35% yield) was obtained in the form of brown-black crystals. Although crystalline **1** appears to noticeably change form and color in the solid state upon drying under vacuum for extended periods of time (e.g., >1 h), this material can still be used for subsequent synthetic reactions. For **1**: H NMR (400 MHz, benzene-d_6, 25 °C) 2.18 (br), 9.05 (br).

(η^5-C_5Me_5)W[(i-Pr)NC(Me)N(i-Pr)]Cl_3 (2). A solution of Li[N(i-Pr)C(Me)N(i-Pr)] (0.225 g, 1.52 mmol in 20 mL of Et_2O) was added dropwise to a solution of (η^5-C_5Me_5)WCl_4 (0.648 mg, 1.41 mmol in 100 mL of Et_2O) at −30 °C over a period of 5 min. The resulting solution was allowed to warm to room temperature and stirred overnight. The solution was then pumped down to a volume of ∼20 mL and filtered through Celite. The volume of the solvent was reduced under vacuum, followed by a second filtration, and then the material was pumped down to dryness. Recrystallization from toluene at −30 °C furnished a blue crystalline material (0.575 g, 72% yield). For **2**: Anal. Calcd for $C_{18}H_{32}Cl_3N_2W$ C, 38.15; H, 5.69; N, 4.94; found C, 37.19; H, 5.60; N, 4.94.

(η^5-C_5Me_5)Mo[(i-Pr)NC(Me)N(i-Pr)]Cl_2 (3). A solution of Li[N(i-Pr)C(Me)N(i-Pr)] (0.836 g, 5.64 mmol in 25 mL of Et_2O) was added dropwise to a solution of (η^5-C_5Me_5)$MoCl_4$ (1.00 g, 2.68 mmol in 175 mL of Et_2O) at −30 °C over a period of 5 min. The resulting solution was allowed to warm to room temperature and stirred overnight. The solution was then pumped down to dryness, extracted in toluene, and filtered through Celite. The volume of the solvent was reduced under vacuum, followed by a second filtration, and then the material was pumped down to dryness. The residue was washed with pentane (2 × 10 mL) and then recrystallized from toluene at −30 °C, furnishing a brownish crystalline material (0. 908 g, 76% yield). For **3**: Anal. Calcd for $C_{18}H_{32}Cl_2N_2Mo$ C, 48.77; H, 7.28; N, 6.32; found C, 48.86; H, 7.38; N, 6.60. ^{1}H NMR (400 MHz, C_6D_6) 2.1 (br), 8.9 (br), 15.8 (br).

(η^5-C_5Me_5)Mo[(i-Pr)NC(NMe_2)N(i-Pr)]Cl_2 (4). A solution of Li[N(i-Pr)C(NMe_2)N(i-Pr)] (0.400 g, 1.60 mmol in 15 mL Et_2O) was added dropwise to a solution of (η^5-C_5Me_5)$MoCl_4$ (0.300 g, 0.804 mmol in 75 mL Et_2O) at −30 °C over a period of 5 min. The resulting solution was allowed to warm to room temperature and stirred overnight. The solution was then pumped down to dryness, extracted in toluene, and filtered through Celite. The volume of the solvent was reduced under vacuum, followed by a second filtration, and then the material was pumped down to dryness. The residue was washed with pentane (2 × 10 mL) and then recrystallized from toluene at −30 °C, furnishing a brownish red crystalline material (0.250 g, 66% yield). For **4**: ^{1}H NMR (400 MHz, C_6D_6) 3.9 (br), 8.1 (br), 11.1 (br), 28.6 (br).

(η^5-C_5Me_5)W[(i-Pr)NC(Me)N(i-Pr)]Cl_2 (5). A solution of **2** (0.200 g, 0.353 mmol in 50 mL Et_2O) was cooled to −30 °C, at which point 0.5% NaHg (1.62 g, 0.352 mmol) was added, and the solution was allowed to warm to room temperature and stirred overnight. The solution was then pumped down to dryness, extracted in toluene, and filtered through Celite. Recrystallization from toluene at −30 °C furnished a brick red crystalline material (0.155 g, 83% yield). For **5**: Anal. Calcd for $C_{18}H_{32}Cl_2N_2W$ C, 40.69; H, 6.07; N, 5.27; found C, 40.69; H, 6.01; N, 5.21. ^{1}H NMR (400 MHz, C_6D_6) 0.94 (6H, d, J = 6.8 Hz, CH(CH_3)$_2$), 1.45 (6H, d, J = 6.8 Hz, CH(CH_3)$_2$), 2.33 (15H, s, C_5(CH_3)$_5$), 3.98 (2H, sp, J = 6.8 Hz, CH(CH$_3$)$_2$), 4.02 (3H, s, NC(CH_3)N).

{(η^5-C_5Me_5)Mo[(i-Pr)NC(Me)N(i-Pr)]}$_2$(μ-η^1:η^1-N_2) (6). i. From Low-Temperature Chemical Reduction of 3 with KC_8. A Schlenk tube equipped with a Teflon valve was charged with **1** (93 mg, 0.21 mmol) and KC_8 (83 mg, 0.61 mmol). The tube was evacuated and cooled to −196 °C, and then THF (10 mL) was added by vacuum transfer. The tube was filled with dinitrogen (1 atm), sealed, and warmed to −78 °C. After stirring at −78 °C for 3 h, the suspension was warmed to 0 °C and stirred for 15 h, followed by warming to room temperature for 5 h. The resulting dark brown/yellow suspension was filtered through Celite, and the solvent was removed under vacuum. The resulting solid was dissolved in a small amount of pentane, filtered, and cooled at −30 °C to afford yellow/brown crystalline material (32 mg, 40%). For **6**: Anal. Calcd for $C_{36}H_{64}N_6Mo_2$ C, 55.95; H, 8.35; N, 10.87; found C, 56.16; H, 8.33; N, 10.85. ^{1}H NMR (400 MHz, C_6D_6) 0.88 (12H, d, J = 6.4 Hz), 1.13 (12H, d, J = 6.4 Hz), 1.87 (30H, s), 1.89 (6H, s), 3.45 (4H, sp, J = 6.4 Hz). Note: due to poor crystallinity and high solubility in pentane, it was not possible to obtain single crystals of **6** that were suitable for X-ray crystallography after several attempts.

Isotopically labeled $^{15}N_2$-**6** was prepared in the same manner as described above under an atmosphere of $^{15}N_2$ (99%). The ^{1}H NMR spectrum was identical to that of unlabeled **6**. For $^{15}N_2$-**6**: ^{15}N NMR (40.5 MHz, benzene-d_6, liq. NH_3 as an external reference) δ 374.9 ppm.

ii. From Chemical Reduction of 1 Using 0.5% NaHg. A solution of **1** (309 mg, 0.700 mmol) in 40 mL of THF was cooled to −30 °C, at which point 0.5% (w/w) of NaHg (13.169 g, 2.864 mmol) was added, and the solution was allowed to warm to room temperature. The reaction mixture was stirred at room temperature for 16 h to yield a yellow-brown colored solution, after which time the volatiles were removed in vacuo and the solid residue was taken up in pentane and filtered through Celite. The filtrate was then concentrated and cooled to −30 °C whereupon 208 mg (77% yield) of **6** was isolated as a yellowish-brown crystalline material.

iii. From Thermolysis of *meso*-11. A NMR tube equipped with a Teflon valve was charged with a solution of *meso*-**11** (36 mg, 0.046 mmol) in benzene-d_6 (1.5 mL). The tube was then heated to 70 °C over a period of 1 week, with the reaction progress being monitored periodically. After this period, the solution was drained from the tube, the tube was rinsed with pentane, and the combined solutions were pumped down to dryness in vacuo. The resulting residue was taken up in a minimal amount of pentane and cooled to −30 °C, which furnished yellow/brown crystals of **6** (19 mg, 51% yield).

{(η^5-C_5Me_5)Mo[N(i-Pr)C(NMe_2)N(i-Pr)]}$_2$(μ-η^1:η^1-N_2) (7). A Schlenk tube equipped with a Teflon valve was charged with **4** (99 mg, 0.21 mmol) and KC_8 (89 mg, 0.66 mmol). The tube was evacuated and cooled to −196 °C, and then THF (10 mL) was

added by vacuum transfer. The tube was filled with dinitrogen (1 atm), sealed, and warmed to −78 °C. After stirring at −78 °C for 5 h, the suspension was warmed to 0 °C and stirred for 15 h, followed by warming to room temperature for 5 h. The resulting dark brown/yellow suspension was filtered through Celite, and the solvent was removed under vacuum. The resulting solid was dissolved in a small amount of pentane, filtered, and cooled to −30 °C to afford yellow/brown crystalline material (33 mg, 38% yield). For **7**: Anal. Calcd for $C_{36}H_{64}N_6Mo_2$ C, 54.93; H, 8.49; N, 13.49; found C, 55.01; H, 8.45; N, 13.29. ^{1}H NMR (400 MHz, C_6D_6) 0.85(12H, d, J = 6.4 Hz, CH(CH_3)$_2$), 1.18 (12H, d, J = 6.4 Hz, CH(CH_3)$_2$), 1.90 (30H, s, C$_5$(CH_3)$_5$), 2.67 (12H, s, N(CH_3)$_2$), 3.67 (4H, sp, J = 6.4 Hz CH(CH$_3$)$_2$).

{(η^5-C$_5$Me$_5$)W[(i-Pr)NC(Me)N(i-Pr)]}$_2$(μ-η^1:η^1-N$_2$) (8). i. From Low-Temperature Chemical Reduction of 2 with KC$_8$. A Schlenk tube equipped with a Teflon valve was charged with **2** (100 mg, 0.176 mmol) and KC$_8$ (95 mg, 0.703 mmol). The tube was evacuated and cooled to −196 °C, and then THF (10 mL) was added by vacuum transfer. The tube was filled with dinitrogen (1 atm), sealed, and warmed to −78 °C. After stirring at −78 °C for 3 h, the suspension was warmed to 0 °C and stirred for 15 h, followed by warming to room temperature for 5 h. The resulting dark green suspension was filtered through Celite, and the solvent was removed under vacuum. The resulting solid was dissolved in a small amount of pentane, filtered, and cooled to −30 °C to afford green crystalline material (47 mg, 56% yield). For **8**: Anal. Calcd for $C_{36}H_{64}N_6W_2$ C, 45.58; H, 6.80; N, 8.86; found C, 45.74; H, 6.81; N, 8.76. ^{1}H NMR (400 MHz, C_6D_6) 0.98 (12H, d, J = 6.4 Hz, CH(CH_3)$_2$), 1.24 (12H, d, J = 6.4 Hz, CH(CH_3)$_2$), 1.71 (6H, s, NC(CH_3)N), 2.14 (30H, s, C$_5$(CH_3)$_5$), 3.26 (4H, sp, J = 6.4 Hz, CH(CH$_3$)$_2$).

The isotopically labeled compound ^{15}N$_2$-**8** was prepared in the same manner as described above under an atmosphere of ^{15}N$_2$ gas. The ^{1}H NMR spectrum was identical to that of unlabeled **8**. For ^{15}N$_2$-**8**: ^{15}N NMR (40.5 MHz, C_6D_6) 351.4 [^1J(^{183}W−^{15}N) = 145 Hz, ^2J(^{183}W−^{15}N) = 10.5 Hz).

ii. From Chemical Reduction of 2 Using 0.5% NaHg. A solution of **2** (0.307 g, 0.54 mmol) in 30 mL of THF was cooled to −30 °C, at which point 0.5% (w/w) Na/Hg (9.964 g, 2.167 mmol) was added and the solution was allowed to warm to room temperature. The reaction mixture was stirred at room temperature for 1.5 h to yield a dark green colored solution, after which time the volatiles were removed in vacuo and the solid residue was taken up in pentane and filtered through Celite. The resulting dark green filtrate was then concentrated and cooled to −30 °C whereupon 257 mg (92% yield) of **8** was isolated as a dark green crystalline material.

(η^5-C$_5$Me$_5$)TiCl$_2$[N(i-Pr)C(Me)N(i-Pr)] (9). To a solution of (η^5-C$_5$Me$_5$)TiCl$_3$ (0.791 g, 2.73 mmol) in Et$_2$O (75 mL) was added Li[N(i-Pr)C(Me)N(i-Pr)] (0.405 g, 2.73 mmol) at −35 °C. The reaction was warmed to ambient temperature and stirred for 16 h, during which time the solution changed in color from orange to burgundy. The solvent was removed in vacuo, and the resulting product was filtered through Celite and recrystallized from toluene (0.939 g, 2.37 mmol, 87% yield). For **9**: ^{1}H NMR (400 MHz, C_6D_6) δ 3.92 (2H, m, CH(CH$_3$)$_2$), 2.05 (15H, s, C$_5$*Me*$_5$), 1.57 (s, 3H, CH_3), 1.14 (12H, d, CH(CH_3)$_2$). Anal, Calcd. for TiC$_{18}$H$_{32}$N$_2$Cl$_2$ C, 54.70; H, 8.16; N, 7.09; found C, 54.74; H, 8.00; N, 7.16.

{(η^5-C$_5$Me$_5$)Ti[N(i-Pr)C(Me)N(i-Pr)]}$_2$(μ-η^1:η^1-N$_2$) (10). A Schlenk tube equipped with a Teflon valve was charged with **9** (102 mg, 0.258 mmol) and KC$_8$ (104 mg, 0.769 mmol). The tube was evacuated and cooled to −196 °C, and then THF (10 mL) was added by vacuum transfer. The tube was filled with dinitrogen (1 atm), sealed, and warmed to −78 °C. After stirring at −78 °C for 3 h, the suspension was warmed to 0 °C and stirred for 15 h, followed by warming to room temperature for 5 h. The resulting dark green suspension was filtered through Celite, and the solvent was removed under vacuum. The resulting solid was dissolved in a small amount of pentane, filtered, and cooled to −30 °C to afford green crystalline material (43 mg, 49% yield). For **10**: Anal. Calcd for $C_{36}H_{64}N_6Ti_2$ C, 63.89; H, 9.53; N, 12.42; found C, 63.40; H, 9.36; N, 11.97. ^{1}H NMR (400 MHz, C_6D_6) 1.01 (12H, d, J = 6.4 Hz, CH(CH_3)$_2$), 1.05 (12H, d, J = 6.4 Hz, CH(CH_3)$_2$), 2.06 (30H, s, C$_5$(CH_3)$_5$), 2.09 (6H, s, NC(CH_3)N), 3.97 (4H, sp, J = 6.4 Hz, CH(CH$_3$)$_2$).

{(η^5- C$_5$Me$_5$)Mo(H)[(i-Pr)NC(Me)N(i-Pr)]}$_2$(μ-η^1:η^1-N$_2$) (*meso*-11). A solution of **1** (110 mg, 0.248 mmol) in Et$_2$O (25 mL) in a screw-cap vial was cooled to −30 °C, and then *n*BuLi (0.30 mL, 1.70 M in hexanes, 0.51 mmol) was added dropwise via syringe. The resulting solution was capped and allowed to warm to room temperature while stirring overnight. The volatiles were removed under vacuum, and the residue was extracted in pentane and filtered through Celite. The volume of the solution was reduced under vacuum, a second filtration was performed, and the resulting solution was cooled to −30 °C to provide brown crystalline material (63 mg, 66% yield). For **11**: Anal. Calcd for $C_{36}H_{66}N_6Mo_2$ C, 55.95; H, 8.35; N, 10.87; found C, 55.65; H, 8.36; N, 10.57. ^{1}H NMR (400 MHz, C_6D_6) −1.51 (2H, s), 1.06 (6H, d, J = 6.4 Hz), 1.09 (6H, d, J = 6.4 Hz), 1.20 (6H, d, J = 6.4 Hz), 1.28 (6H, d, J = 6.4 Hz), 1.60 (6H, s), 1.99 (30H, s), 3.50 (4H, m).

{(η^5-C$_5$Me$_5$)W(Cl)[(i-Pr)NC(Me)N(i-Pr)]}$_2$(μ-η^1:η^1-N$_2$) (*rac,meso*-12). A Schelnk tube equipped with a Teflon valve was charged with **8** (45 mg, 0.047 mmol) and PbCl$_2$ (13 mg, 0.047 mmol). The tube was evacuated and cooled to −196 °C, and then Et$_2$O (5 mL) was added by vacuum transfer. The tube was warmed to room temperature and stirred for 18 h, at which point it was pumped down to dryness, then extracted with pentane and filtered through Celite. The resulting yellow/brown solution was reduced in volume, refiltered, and cooled to −30 °C to afford dark yellow crystalline material (40 mg, 83% yield), which was seen to be a 1:1 mixture of two diastereomers that were not readily separable by fractional crystallization. For **12**: Anal. Calcd for $C_{36}H_{64}N_6Cl_2W_2$ C, 42.41; H, 6.33; N, 8.24; found C, 42.60; H, 6.26; N, 8.26. ^{1}H NMR (400 MHz, C_6D_6) 1.11 (6H, d, J = 6.8 Hz, CH(CH_3)$_2$), 1.21 (6H, d, J = 6.8 Hz, CH(CH_3)$_2$), 1.24 (6H, d, J = 6.8 Hz, CH(CH_3)$_2$), 1.25 (6H, d, J = 6.8 Hz, CH(CH_3)$_2$), 1.27 (6H, d, J = 6.8 Hz, CH(CH_3)$_2$), 1.32 (6H, d, J = 6.8 Hz, CH(CH_3)$_2$), 1.34 (6H, d, J = 6.8 Hz, CH(CH_3)$_2$), 1.61 (6H, d, J = 6.8 Hz, CH(CH_3)$_2$), 1.66 (6H, s, NC(CH_3)N), 1.80 (6H, s, NC(CH_3)N), 2.05 (30H, s, C$_5$(CH_3)$_5$), 2.10 (30H, s, C$_5$(CH_3)$_5$), 3.71 (2H, sp, J = 6.8 Hz, CH(CH$_3$)$_2$), 3.82 (2H, sp, J = 6.8 Hz, CH(CH$_3$)$_2$), 4.07 (2H, sp, J = 6.8 Hz, CH(CH$_3$)$_2$), 4.18 (2H, sp, J = 6.8 Hz, CH(CH$_3$)$_2$).

(η^5-C$_5$Me$_5$)Mo[N(i-Pr)C(Me)N(i-Pr)](CNAr)$_2$ (Ar = 3,5-Me$_2$-C$_6$H$_3$) (13). A flask was charged with **6** (32 mg, 0.041 mmol), 2,6-dimethylphenylisocyanide (20 mg, 0.16 mmol), and toluene (2 mL), and the mixture was stirred at room temperature for 18 h, over which time the solution turned a deep green. The solution was pumped down to dryness under vacuum, taken up in pentane, and filtered through Celite. The pentane solution was cooled to −30 °C to afford green crystalline material (38 mg, 93% yield). For **13**: Anal. Calcd for $C_{36}H_{50}N_4Mo$ C, 68.12; H, 7.94; N, 8.83; found C, 67.61; H, 7.68; N, 8.39. ^{1}H NMR (400 MHz, C_6D_6) 1.05 (6H, d, J = 6.4 Hz), 1.19 (6H, d, J = 6.4 Hz), 1.58 (3H, s), 1.88 (15H, s), 2.43 (12H, s), 3.61 (4H, sp, J = 6.4 Hz), 6.746 (2H, t, J = 7.6 Hz), 6.89 (4H, d, J = 7.6 Hz). ^{13}C NMR (125.8 MHz, C_6D_6) 11.9, 14.7, 20.3, 23.2, 25.9, 49.9, 105.2, 124.3, 132.2, 134.8, 167.1, 247.5. IR (pentane) ν_{CN} = 1966 cm^{-1}(s), 1971 cm^{-1}(s).

(η^5-C$_5$Me$_5$)W[N(i-Pr)C(Me)N(i-Pr)](CNAr)$_2$ (Ar = 3,5-Me$_2$C$_6$H$_3$) (14). A flask was charged with **8** (25 mg, 0.026 mmol), 2,6-dimethylphenylisocyanide (13 mg, 0.11 mmol), and toluene (2 mL), and the mixture was stirred at room temperature for 18 h, over which time the solution turned a darker green. The solution was pumped down to dryness under vacuum, taken up in pentane, and filtered through Celite. The pentane solution was cooled to −30 °C to afford green crystalline material (27 mg, 73% yield). For **14**: Anal. Calcd for $C_{36}H_{50}N_4W$ C, 59.83; H, 6.97; N, 7.75; found C, 59.37; H, 7.07; N, 7.56. ^{1}H NMR (400 MHz, C_6D_6) 1.04 (6H, d, J = 6.4 Hz), 1.14 (6H, d, J = 6.4 Hz), 1.51 (3H, s), 1.92 (15H, s),

2.50 (12H, s), 3.52 (4H, sp, $J = 6.4$ Hz), 6.74 (2H, t, $J = 7.6$ Hz), 6.96 (4H, d, $J = 7.6$ Hz). ^{13}C NMR (125.8 MHz, C_6D_6) 12.0, 14.7, 20.7, 25.3, 25.8, 50.0, 103.5, 124.4, 128.8, 135.5, 137.3, 168.0, 244.3. IR (pentane) $\nu_{CN} = 1940$ cm^{-1}(s), 1952 cm^{-1}(s).

(η^5-C_5Me_5)Mo[N(i-Pr)C(Me)N(i-Pr)](CO)$_2$ (15). Within a Schlenk tube, a solution of **6** (0.142 g, 0.184 mmol) in 6 mL of toluene was charged with 5 psi of carbon monoxide (99.95%), and the contents of the storage tube were stirred for 40 h at room temperature. The volatiles from the resulting dark red solution were then removed in vacuo, and the residue was taken up in pentane and filtered through a pad of Kimwipe placed within a glass pipet. The solvent of the dark red filtrate was removed in vacuo to provide a dark red solid that was recrystallized from pentane at −30 °C to provide **15** (0.112 g, 71% yield). For **15**: Anal. Calcd for $C_{20}H_{32}N_2O_2Mo$ C, 56.05; H, 7.53; N, 6.54; found C, 56.57; H, 7.38; N, 6.54. ^{1}H NMR (400 MHz, C_6D_6) 0.99 (6H, d, $J = 6.3$ Hz), 1.03 (6H, d, $J = 6.3$ Hz), 1.42 (3H, s), 1.74 (15H, s), 3.48 (2H, sp, $J = 6.3$ Hz). IR (KBr) $\nu_{CO} = 1909$ and 1806 cm^{-1}.

(η^5-C_5Me_5)W[N(i-Pr)C(Me)N(i-Pr)](CO)$_2$ (16). Within a Schlenk tube, a solution of **8** (60 mg, 63 μmol) in 4 mL of toluene was charged with 5 psi of carbon monoxide (99.95%), and the contents of the storage tube were stirred for 40 h at room temperature. The volatiles from the resulting dark brown solution were then removed in vacuo, and the residue taken up in pentane and filtered through a pad of Kimwipe placed within a glass pipet. The solvent of the dark brown filtrate was removed in vacuo to provide a brown solid that was recrystallized from pentane containing a few drops of toluene at −30 °C to provide **16** as orange-red crystals (39 mg, 59% yield). For **16**: Anal. Calcd for $C_{20}H_{32}N_2O_2W$ C, 46.34; H, 6.22; N, 5.40; found C, 46.19; H, 6.11; N, 5.37. ^{1}H NMR (400 MHz, C_6D_6) 0.99 (6H, d, $J = 6.4$ Hz), 1.01 (6H, d, $J = 6.4$ Hz), 1.34 (3H, s), 1.81 (15H, s), 3.35 (2H, sp, $J = 6.4$ Hz). IR (KBr) $\nu_{CO} = 1892$ and 1788 cm^{-1}.

Acknowledgment. Funding for this work was provided by the Department of Energy, Basic Energy Sciences (Grant DE-SC0002217), and in part, by the NSF (Grant CHE-0848293), for which we are grateful.

Supporting Information Available: Details of single-crystal X-ray analyses, including tables of bond lengths and angles, and anisotropic displacement parameters for the solid-state structures, and complete X-ray crystallographic data (CIF) for compounds **3**, **4**, **7**, **8**, **10**, *meso*-**11**, *rac*-**12**, *meso*-**12**, **13**, **14**, **15**, and **16**. This material is available free of charge via the Internet at http://pubs.acs.org.

JA100469F